Contents

Wind-Driven Circulation

We will now use and integrate both Ekman theory and the geostrophic approximation to get a first solution to the wind-driven circulation. They will be the basis for the theory of the wind-driven gyres. At first, the theory will be simple, with no topography and in a steady state, but it will be able to explain many of the qualitative features of the wind-driven circulation.

The first theory presented is the steady, forced-dissipative, homogeneous model first formulated by Stommel; and different versions will be discussed.

We start with the simplest model that can capture our physical setting. We will assume (see Fig. 7.1)

- a homogeneous (or depth-integrated) model.

- Flat bottom.

- Steady state.

- The β-plane approximation.

Let's now remember the solutions for the top and bottom Ekman vertical velocities, and the momentum equations for the geostrophic flow:

$$w_E^T = \frac{1}{f_0}\left(\partial_x \tilde{\tau}^y - \partial_y \tilde{\tau}^x\right) = \frac{1}{f_0}\,\mathrm{curl}_z\,\tilde{\boldsymbol{\tau}}_T \;\; = \;\; \frac{1}{\rho_0 f_0}\mathrm{curl}_z\,\boldsymbol{\tau}_T \qquad (7.1)$$

$$w_E^B = -\frac{1}{\rho_0}\nabla\cdot\boldsymbol{M}_E = \frac{1}{f_0}\,\mathrm{curl}_z\,\tilde{\boldsymbol{\tau}}_B \;\; = \;\; \frac{d}{2}\zeta_g, \qquad (7.2)$$

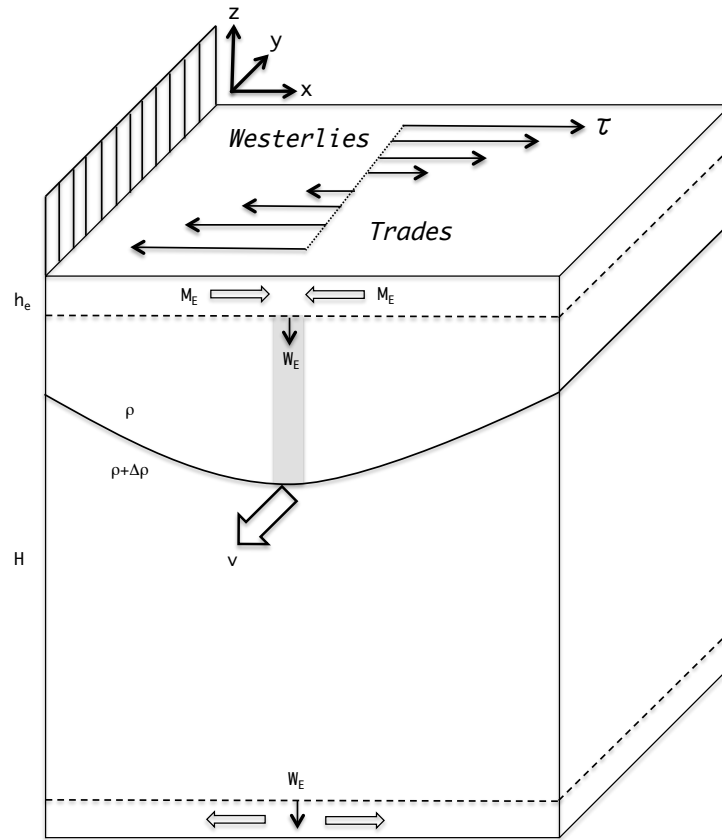where $\zeta_g = (\partial_x v_g - \partial_y u_g)$ is the vorticity of the interior geostrophic flow.

Figure 7.1: *A schematic of an idealized wind-driven Ekman pumping on a β-plane for a homogeneous ocean of depth H, resulting in a simple model for mid-latitude ocean circulation.*

The interior geostrophic flow (for a homogeneous barotropic fluid in which $\rho' = 0$) is

$$-fv = -\frac{1}{\rho_0} \frac{\partial p}{\partial x} \tag{7.3}$$

$$fu = -\frac{1}{\rho_0} \frac{\partial p}{\partial y} \tag{7.4}$$

$$0 = \frac{1}{\rho_0} \frac{\partial p}{\partial z} \tag{7.5}$$

$$\frac{\partial u}{\partial x} + \frac{\partial v}{\partial y} + \frac{\partial w}{\partial z} = 0 \tag{7.6}$$

7.1 A linear geostrophic vorticity balance approach: Sverdrup Balance

Within a β-plane, the interior geostrophic flow becomes

$$-(f_0 + \beta y)v = -\frac{1}{\rho_0}\frac{\partial p}{\partial x} \tag{7.7}$$

$$(f_0 + \beta y)u = -\frac{1}{\rho_0}\frac{\partial p}{\partial y} \tag{7.8}$$

$$0 = \frac{1}{\rho}\frac{\partial p}{\partial z} \tag{7.9}$$

$$\nabla_3 \cdot v = 0. \tag{7.10}$$

And we will use $v = (u, v, w)$ and $\boldsymbol{u} = (u, v)$.

Cross-differentiating the horizontal momentum equations $[\partial_x(7.8)\text{-}\partial_y(7.7)]$ gives:

$$f_0\left(\frac{\partial u}{\partial x} + \frac{\partial v}{\partial y}\right) + \beta y\left(\frac{\partial u}{\partial x} + \frac{\partial v}{\partial y}\right) + \beta v = 0. \tag{7.11}$$

But since in a β-plane $\beta y \ll f_0$, we have

$$f_0\left(\frac{\partial u}{\partial x} + \frac{\partial v}{\partial y}\right) + \beta v = 0. \tag{7.12}$$

or

$$\boxed{\beta v = f_0 \frac{\partial w}{\partial z}} \tag{7.13}$$

Which is a form of the linear geostrophic vorticity balance, and is known as **SVERDRUP BALANCE**.

Eq.7.13 expresses a conservation of potential vorticity. If $\frac{\partial w}{\partial z} > 0$, there will be stretching of the fluid column. *As the column stretches and shrinks it has to increase its vorticity in order to conserve angular momentum.* At large scales, the only significant vorticity is the planetary vorticity f, which in this case has to increase to balance the positive $\frac{\partial w}{\partial z}$. β is indeed a rate of vorticity change $\left(\frac{\partial f}{\partial y}\right)$. This balance is responsible for a meridional velocity v.

Geostrophy was previously studied on a f-plane, resulting in $w = 0$. We now find a vertical velocity within the geostrophic flow using the β-plane. If $\beta = 0 = \frac{\partial f}{\partial y}$, then the vertical geostrophic velocity is $w = 0$.

What is the structure of $\frac{\partial w}{\partial z}$?

Taking the vertical derivative of the horizontal momentum equations

$$-(f_0 + \beta y)\frac{\partial v}{\partial z} = -\frac{1}{\rho_0}\frac{\partial^2 p}{\partial x \partial z} \tag{7.14}$$

$$(f_0 + \beta y)\frac{\partial u}{\partial z} = -\frac{1}{\rho_0}\frac{\partial^2 p}{\partial y \partial z}. \tag{7.15}$$

But $\frac{\partial p}{\partial z} = 0$. Hence $\frac{\partial u}{\partial z} = \frac{\partial v}{\partial z} = 0$ and the flow is barotropic and there is no vertical shear. $\frac{\partial w}{\partial z}$ is constant throughout the interior and different from zero.

Now take a vertical derivative of the vertical velocity, and remembering the Ekman solutions we find

$$\frac{\partial w}{\partial z} = \frac{w_T - w_B}{H} = \frac{1}{\rho_0 f_0 H}curl_z\tau - \frac{d}{2H}\zeta_g, \tag{7.16}$$

where H is the depth of the interior flow.

Using the geostrophic expressions for the horizontal velocities

$$-\frac{\partial v}{\partial x} = -\frac{1}{\rho_0 f_0}\frac{\partial^2 p}{\partial x^2} \tag{7.17}$$

$$\frac{\partial u}{\partial y} = -\frac{1}{\rho_0 f_0}\frac{\partial^2 p}{\partial y^2} \tag{7.18}$$

our solution $\beta v = f_0\frac{\partial w}{\partial z}$ becomes

$$\frac{\beta}{\rho_0 f_0^2}\frac{\partial p}{\partial x} = \frac{1}{\rho_0 f_0 H}curl_z\tau - \frac{d}{2H\rho_0 f_0}\left(\frac{\partial^2 p}{\partial x^2} + \frac{\partial^2 p}{\partial y^2}\right), \tag{7.19}$$

since $\zeta = \left(\frac{\partial v}{\partial x} - \frac{\partial u}{\partial y}\right)$. Or

$$\boxed{\underbrace{\beta\frac{\partial p}{\partial x}}_{\text{meridional velocity}} = \frac{f_0}{H}\Big(\underbrace{curl_z\tau}_{\substack{\text{Ekman at} \\ \text{the top}}} - \underbrace{\frac{d}{2}\nabla^2 p}_{\substack{\text{Ekman at} \\ \text{the bottom}}}\Big)} \tag{7.20}$$

This is the governing equation for the ocean interior, away from the Ekman layers. It is driven by input of momentum at the surface and drag at the bottom.
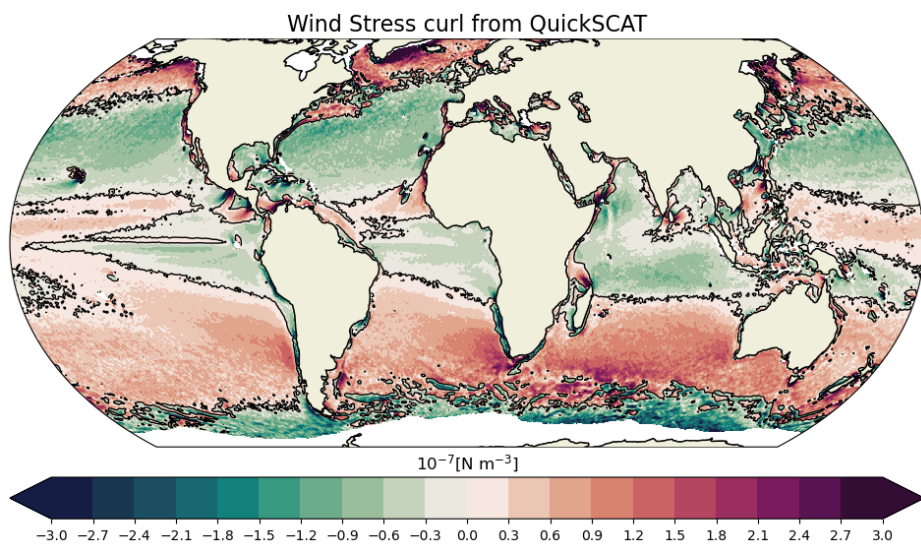
Figure 7.2: *Wind stress curl computed from QuickSCAT reanalysis [https://doi.org/10.1175/2008JPO3881.1].*

7.2 The Stommel model

We will now use the planetary-geostrophic equations. Let's define $\phi = p/\rho_0$ and $b = -g\rho'/\rho_0$. For a Boussinesq fluid, the planetary geostrophic equations are

$$\mathbf{f} \times \mathbf{u} = -\nabla\phi + \frac{1}{\rho_0}\frac{\partial\tau}{\partial z} \tag{7.21}$$

$$\frac{\partial\phi}{\partial z} = b \tag{7.22}$$

$$\nabla_3 \cdot \mathbf{v} = 0. \tag{7.23}$$

The first equation is the horizontal momentum equation using geostrophic balance and a stress term. The second equation is the vertical momentum equation (hydrostatic balance). And the third is mass continuity.

The planetary geostrophic equations are essentially the Boussinesq primitive equations with the advection terms omitted in the horizontal momentum equation. They have been derived with a 'low Rossby number scaling', but for large scales, much larger than the deformation scale. Hence, this set of equations are composed of the geostrophic balance and the full mass continuity equations. These equations are not too useful in the atmosphere, where the deformation radius for a continuously stratified fluid, $L_d = \frac{NH}{f}$ (or $\frac{\sqrt{gH}}{f}$), is about 1000 km. Only the description of planetary waves can satisfy the PG equations. For the ocean, instead, where $L_d \simeq 100$ km, the PG equations are very useful, and used for the theory of large-scale circulation.

We now take the curl (or cross-differentiate) of (7.21) and find

$$\mathbf{f}\nabla \cdot \mathbf{u} + \frac{\partial f}{\partial y}v = curl_z\widetilde{\tau} \tag{7.24}$$

where again $curl_z A = \mathbf{k} \cdot \nabla \times A = \partial_x A^y - \partial_y A^x$, and $\widetilde{\tau} = \tau/\rho_0$.

Now integrate over the full depth of the ocean

$$\int \mathbf{f}\nabla \cdot \mathbf{u}\,\mathrm{d}z + \frac{\partial f}{\partial y}\int v\,\mathrm{d}z = curl_z(\widetilde{\tau}_T - \widetilde{\tau}_B). \tag{7.25}$$

The first term vanishes, the divergence term, if the vertical velocities are zero at the top and bottom of the ocean. This is true for a flat-bottomed ocean but is not the case when topography will be added. We are thus left with:

$$\boxed{\beta\overline{v} = curl_z(\widetilde{\tau}_T - \widetilde{\tau}_B)}. \tag{7.26}$$

Where $\overline{A} = \int A\,dz$. Eq. (7.26) is equivalent to Eq. (7.13), i.e. the SVER-DRUP BALANCE, *a balance between the input of vorticity from the wind-stress curl and the advection of planetary vorticity.*

We now work on the rhs of (7.26). At the top the stress is given by the wind. At the bottom, which is flat for now, we parameterize the stress with a LINEAR DRAG, or Rayleigh friction, as it would be generated by an Ekman layer, and obtain

$$\boxed{\beta \overline{v} = F_\tau(x, y) - r\overline{\zeta}}. \tag{7.27}$$

Here the meridional flow is governed by

1. $F_\tau(x, y) = curl_z \widetilde{\tau}_T$; the curl of the wind stress at the top of the ocean.

2. $\overline{\zeta} = \frac{\partial \overline{v}}{\partial x} - \frac{\partial \overline{u}}{\partial y}$; the vorticity of the vertically integrated flow

3. r; a linear drag or Rayleigh friction.

The flow velocity is divergent-free and we can define a streamfunction

$$\overline{u} = -\frac{\partial \psi}{\partial y} \quad \overline{v} = \frac{\partial \psi}{\partial x}$$

such that

$$\boxed{\beta \frac{\partial \psi}{\partial x} = F_\tau(x, y) - r\nabla^2 \psi}. \tag{7.28}$$

This is the **STOMMEL PROBLEM or MODEL**. The contribution of Stommel is the addition of a linear bottom drag that would balance the momentum input at the surface.

7.2.1   A homogeneous model

Instead of vertically integrating our momentum equations, we can instead consider a homogeneous layer of fluid, obeying the shallow water equations. The potential vorticity equation becomes

$$\frac{D}{Dt}\left(\frac{f + \zeta}{H}\right) = \frac{F}{H}, \tag{7.29}$$

where F represents both forcing and friction. If the ocean is flat-bottomed and has a rigid lid, then

$$\frac{D\zeta}{Dt} + \beta v = F. \tag{7.30}$$

This is the barotropic PV equation. Because of the rigid lid and flat-bottom, the flow is divergent-free, and we can express it with the usual streamfunction:

$$\boxed{\frac{\mathrm{D}}{\mathrm{D}t}\nabla^2\psi + \beta\frac{\partial\psi}{\partial x} = F_\tau(x,y) - r\nabla^2\psi}. \tag{7.31}$$

The first term of the l.h.s characterizes the *time-dependent, non-linear* STOMMEL MODEL. The steady non-linear model is simply

$$J(\psi,\nabla^2\psi) + \beta\frac{\partial\psi}{\partial x} = F_\tau(x,y) - r\nabla^2\psi. \tag{7.32}$$

Where the Jacobian is

$$J(A,B) = \frac{\partial A}{\partial x}\frac{\partial B}{\partial y} - \frac{\partial A}{\partial y}\frac{\partial B}{\partial x}. \tag{7.33}$$

And so the advective term is

$$u\frac{\partial\nabla^2\psi}{\partial x} + v\frac{\partial\nabla^2\psi}{\partial y} \quad = \tag{7.34}$$

$$-\frac{\partial\psi}{\partial y}\frac{\partial\nabla^2\psi}{\partial x} + \frac{\partial\psi}{\partial x}\frac{\partial\nabla^2\psi}{\partial y} \quad = \tag{7.35}$$

$$\frac{\partial\psi}{\partial x}\frac{\partial\nabla^2\psi}{\partial y} - \frac{\partial\psi}{\partial y}\frac{\partial\nabla^2\psi}{\partial x} \quad = \tag{7.36}$$

$$J(\psi,\nabla^2\psi). \tag{7.37}$$

To recover the original Stommel model we need to ignore the advective derivative (the source of our non-linearities).

Take the barotropic PV equation (7.30) and perform a scale analysis of all terms:

$$\underbrace{\frac{\mathrm{D}\zeta}{\mathrm{D}t}}_{\frac{U}{L}\frac{U}{L}} + \underbrace{\beta v}_{\beta U} = F. \tag{7.38}$$

Let's define $Z = \frac{U}{L}$ a representative value for vorticity, so that in order to ignore nonlinearities the following inequality must hold: $Z \ll \beta L$, or

$$R_\beta = \frac{U}{\beta L^2} \ll 1 \tag{7.39}$$

which is called the β Rossby number[1]. Assuming a β Rossby number much smaller than unity is equivalent to the small Rossby number assumption used to obtain the PG equations.

---

[1]Remember that the Rossby number is $R_o = \frac{U}{fL}$

The response to an input of vorticity: relative vorticity or planetary vorticity?

Recalling the PV equation

$$\frac{D}{Dt}\left(\frac{f+\zeta}{H}\right) = \frac{F}{H},\tag{7.40}$$

The ocean will respond to an input of vorticity F by either changing ζ or f. Using the above scaling approach we see that

$$\underbrace{\frac{D\zeta}{Dt}}_{\frac{U^2}{L^2}} + \underbrace{\beta v}_{\beta U} = F.\tag{7.41}$$

The ratio of relative vorticity and advection of planetary vorticity is

$$\frac{D\zeta}{Dt}\bigg/\frac{Df}{Dt} \sim \frac{U}{\beta L^2} \equiv R_\beta.\tag{7.42}$$

- Consider now the basin scale ($L \sim 1000$ km, $U \sim 0.01$ m s^{-1}). The β Rossby number would be

$$R_\beta = \frac{U}{\beta L^2} = \frac{10^{-2}}{10^{-11}(10^6)^2} = 10^{-3}.\tag{7.43}$$

  Within the basin scale, the rate of change of relative vorticity is small compared to the rate of change of planetary vorticity. This means that an input of vorticity, say from the wind, does not induce the flow to increase its rotation, rather it will force the flow to move meridionally to reach a balance through f.

- Now consider a frontal zone instead ($L \sim 10$ km, $U \sim 0.1$ m s^{-1}). The β Rossby number would be

$$R_\beta = \frac{U}{\beta L^2} = \frac{10^{-1}}{10^{-11}(10^4)^2} = 10^2.\tag{7.44}$$

  Within a frontal zone, the rate of change of ζ is much larger than β. This means that the ocean will respond to F by changing ζ.

The response is thus fundamentally different, and the two regions will be governed by different dynamics: there will be a large *interior* regime and a narrow *boundary layer* regime.

7.2.2 The interior: Sverdrup balance

The Stommel model is linear, and we can obtain analytical solutions

$$\boxed{\beta\frac{\partial \psi}{\partial x} = F_\tau(x,y) - r\nabla^2\psi}$$
(7.45)

First, note that the Stommel model was previously derived by the β-plane approximation to the primitive equations:

$$\beta\frac{\partial p}{\partial x} = \frac{f_0}{H}curl_z\boldsymbol{\tau} - \frac{f_0 d}{2H}\nabla^2 p.$$
(7.46)

Now, let's have a look at the relative role of the top and bottom Ekman contributions. The ratio between the pressure gradient term and the frictional term is

$$\frac{f_0 d}{2H}P/L^2/(\beta P/L) \rightarrow \frac{f_0 d}{2H\beta L}$$
(7.47)

Typical values can be used for $d \sim 15$ m, $f_0 \sim 10^{-4}$, $\beta \sim 10^{-11}$, $H \sim 3000$ m and $L \sim 1000$ km, and the ratio is ~ 0.02. This implies that the frictional term can be neglected and that the Ekman pumping induced by the wind stress is much larger than the one resulting from bottom friction.

This approximation will lead us towards our first solution

$$\beta\frac{\partial p}{\partial x} = \frac{f_0}{H}curl_z\tau,$$
(7.48)

which implies a meridional velocity that is a function of the wind-stress curl, and is best known as *Sverdrup balance*.

Suppose, in fact, that the frictional term is small, so there is an approximate balance between the input of vorticity by the wind stress and the β-effect (or the rate of change of planetary vorticity).

Friction is small if

$$|r\zeta| \ll |\beta v|.$$
(7.49)

If we define $r = \frac{f_0\delta}{H}$, as suggested by (7.46), where δ is the thickness of the bottom Ekman layer, then

$$\frac{f_0\delta}{H}\frac{U}{L} \ll \beta U, \quad \text{or} \quad \frac{r}{L} \ll \beta.$$
(7.50)

This inequality is well satisfied in large-scale flows, where L is the horizontal scale of the motion. The vorticity equations is thus

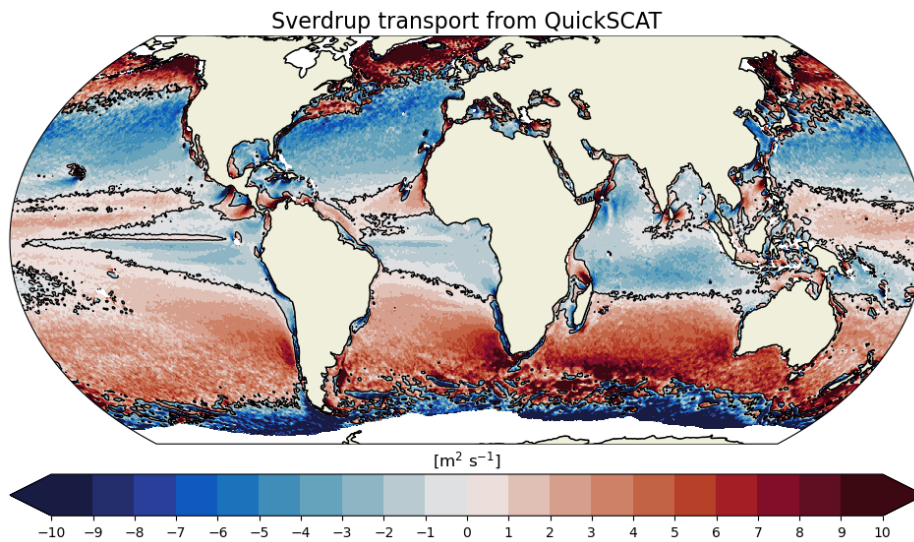$$\beta\frac{\partial \psi}{\partial x} = F_\tau(x,y)$$
(7.51)

Figure 7.3: *Estimate of Sverdrup transport computed from QuickSCAT as* $\overline{v} = curl_z \widetilde{\tau} / \beta$.

which is just an expression of Sverdrup balance

$$\boxed{\beta \overline{v} = curl_z \widetilde{\tau}} \tag{7.52}$$

This is equivalent to the linear geostrophic vorticity balance

$$\beta v = f_0 \frac{\partial w}{\partial z} \tag{7.53}$$

where stress at the bottom is neglected. In fact, over most of the ocean, the deep flow is very weak, meaning that bottom drag is negligible.

Eq.7.52 is not a transport, rather just a balance between wind stress at the surface and the β-effect leading to a meridional velocity $\overline{v} = \frac{1}{\beta} curl_z \tau$ (Fig. 7.3).
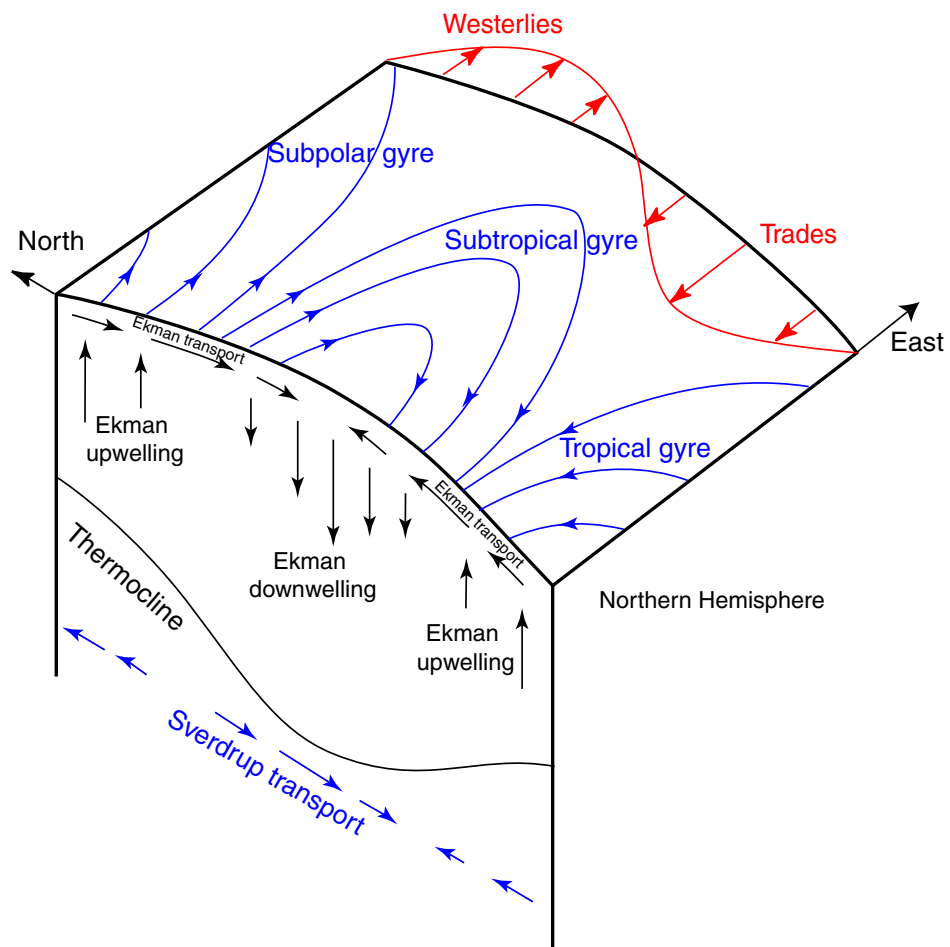
Figure 7.4: *Sverdrup balance circulation ($f > 0$). [from Talley et al. (2011)]*

Physical interpretation

Consider a schematic of the subtropical North Pacific. The winds at the sea surface are not spatially uniform. South of about 30°N, the Pacific is dominated by easterly trade winds. North of this, it is dominated by the westerlies. This causes northward Ekman transport under the trade winds, and southward Ekman transport under the westerlies. As a result, there is Ekman convergence throughout the subtropical North Pacific.

The convergent surface layer water in the subtropics must go some-where so there is downward vertical velocity at the base of the (50 m thick) Ekman layer. At some level between the surface and ocean bottom, there is likely no vertical velocity. Therefore there is net "squashing" of the water columns in the subtropical region (*Ekman pumping*).

This squashing requires a decrease in either planetary or relative vorticity (remember potential vorticity conservation $\frac{D}{Dt}\frac{f+\zeta}{H} = 0$). In the ocean interior, relative vorticity is small, so planetary vorticity must decrease, which results in the equatorward flow that characterizes the subtropical gyre (Fig. 7.4).

The subpolar North Pacific lies north of the westerly wind maximum at about 40°N. Ekman transport is therefore southward, with a maximum at about 40°N and weaker at higher latitudes. Therefore there must be upwelling (*Ekman suction*) throughout the wide latitude band of the subpolar gyre. This upwelling stretches the water columns, which then move poleward, creating the poleward flow of the subpolar gyre.

The Sverdrup transport is the net meridional transport diagnosed in both the subtropical and subpolar gyres, resulting from *planetary vorticity changes that balance Ekman pumping or Ekman suction*. All of the meridional flow is returned in western boundary currents, for reasons described in the following sections. Therefore, subtropical gyres must be anticyclonic and subpolar gyres must be cyclonic.

Computing the transport

Assuming the ocean circulation is in Sverdrup balance, $\bar{v} = \frac{\partial \psi}{\partial x}$ gives the meridional mass transport of the vertically integrated column of fluid due to a surface wind stress. The constraint that there be no normal flow across the ocean's horizontal boundaries means that $\psi = const$ on the boundaries. We pick this constant arbitrarily to be 0. We must choose whether to choose the eastern or western boundary as the limit of integration. This cannot be determined by Sverdrup balance alone, it requires consideration of frictional boundary layers.

We choose the eastern boundary, requiring closure of the circulation in a western boundary current, and we require that the streamfunction be zero on the eastern boundary.

Integrating from east to west, and using the boundary condition $\psi = 0$ at $x = x_E(y)$, the streamfunction is (see Fig. 7.5 and Fig. 7.6)

$$\int_x^{x_E} \frac{\partial \psi}{\partial x}\, dx' = \frac{1}{\beta} \int_x^{x_E} curl_z \widetilde{\tau}_T\, dx$$

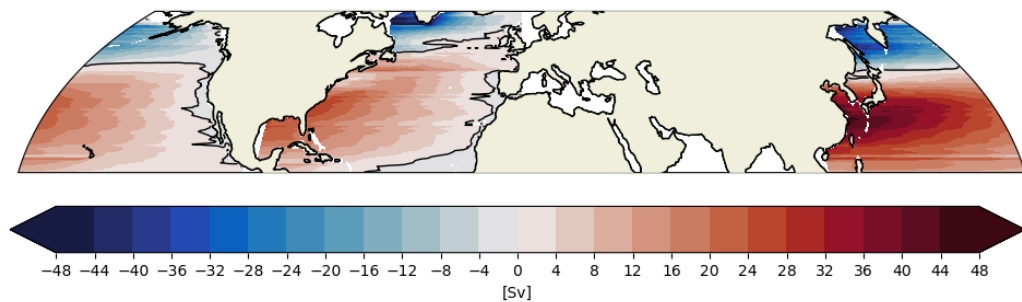$$\psi(x,y) = -\frac{1}{\beta} \int_x^{x_E} curl_z \widetilde{\tau}_T\, dx.$$

Figure 7.5: *Estimate of the depth-integrated circulation (in Sv) predicted by the Sverdrup balance in the North Atlantic and the North Pacific computed with QuickSCAT winds. The solution assumes that the depth-integrated circulation vanishes at the eastern boundary. Positive values (red) correspond to clockwise circulations and negative values (blue) to anticlockwise circulations.*

Two examples are shown in Fig. 7.5 for the North Atlantic and the North Pacific. The Sverdrup balance gives a reasonable good estimation for the interior flow, but a western boundary current is needed to close the circulation. The Sverdrup balance integration results in a realistic large-scale gyre circulation in the tropical, subtropical and subpolar oceans (Fig. 7.6). However something is not well represented and totally missed by the Sverdrup flow. Sverdrup flow predicts an interior flow in balance with the input of vorticity by the wind stress; but the interior meridional flow must be compensated at some level somewhere to comply with mass conservation. This, we will see, is accomplished by a narrow and intense boundary current.

In the Southern Ocean, the zonal integration of the Sverdrup balance does not apply. We will see in Chapter 8 what is so special about the Southern Ocean.
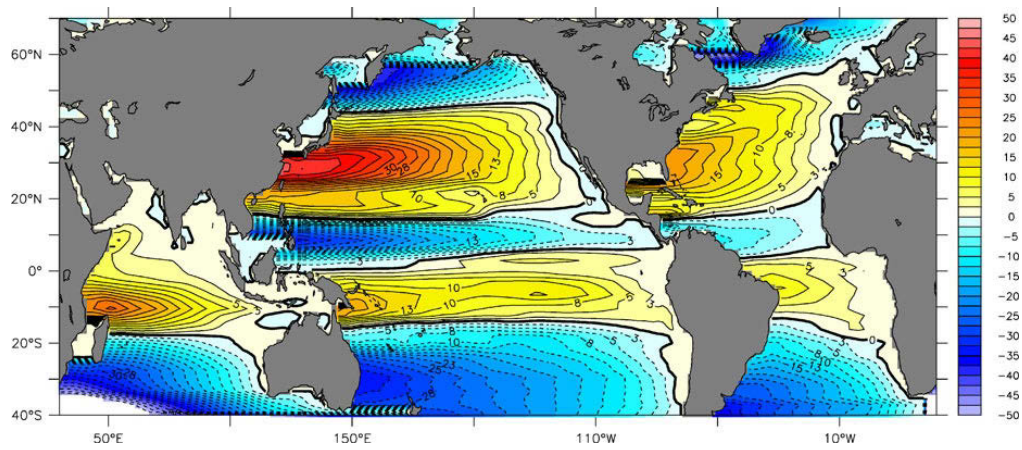
Figure 7.6: *Streamfunction ψ (Sv $\equiv 10^6 \ m^3 \ s^{-1}$) calculated from the Sverdrup relation and a climatological wind stress curl. Westward integration starts at $30°$ E with $\psi = 0$ as boundary condition. [from Olbers et al. (2012)]*

7.2.3 The boundary: Adding a return flow

We need to close the circulation induced by the interior Sverdrup flow. The interior flow was developed for the large scale. We can thus suppose that the return flow will occur in a narrow boundary layer somewhere. Where will this be? Western or eastern side of the basin?

Take the full Stommel model

$$\beta \frac{\partial \psi}{\partial x} = curl_z \boldsymbol{\tau}_T - r\nabla^2 \psi. \tag{7.54}$$

and consider a square domain of side L and rescale variables as follows

$$x = L\,\hat{x} \quad \tau = \tau_0\,\hat{\tau}$$
$$y = L\,\hat{y} \quad \psi = \frac{\tau_0}{\beta}\,\hat{\psi}$$

Hatted variables are non-dimensional and they are $\mathcal{O}(1)$ quantities in the interior.

The Stommel model becomes

$$\beta \frac{\partial \hat{\psi}}{\partial \hat{x}} \frac{\tau_0}{\beta L} = curl_z \hat{\boldsymbol{\tau}}_T \frac{\tau_0}{L} - r\nabla^2 \hat{\psi} \frac{\tau_0}{\beta L^2}$$
$$\frac{\partial \hat{\psi}}{\partial \hat{x}} = curl_z \hat{\boldsymbol{\tau}}_T - \frac{r}{\beta L}\nabla^2 \hat{\psi}$$

which is

$$\frac{\partial \hat{\psi}}{\partial \hat{x}} = curl_z \hat{\boldsymbol{\tau}}_T - \epsilon_s \nabla^2 \hat{\psi} \tag{7.55}$$

where $\epsilon_s = \frac{r}{\beta L} \ll 1$, as shown by (7.50), for the large-scale flow. We thus write a solution for the interior, where friction is small, and a solution for the boundary, where frictional effects will be large:

$$\psi(x,y) = \psi_I(x,y) + \phi(x,y)$$

where ϕ is a boundary layer correction.

The interior solution

In the interior the flow is described by $\psi_I(x,y)$ in the limit where $\epsilon_s = \frac{r}{\beta L} \ll 1$

$$\frac{\partial \psi_I}{\partial x} = curl_z \boldsymbol{\tau}_T \tag{7.56}$$

The solution of the Sverdrup interior is

$$\psi_I(x,y) = \int_0^x curl_z\boldsymbol{\tau}(x',y)\mathrm{d}x' + g(y) \tag{7.57}$$

where $g(y)$ is an arbitrary function. Given the streamfunction definition ($v_I = \partial\psi_I/\partial x$; $u_I = -\partial\psi_I/\partial y$), the corresponding velocities are

$$v_I = curl_z\boldsymbol{\tau}$$
$$u_I = -\partial_y \int_0^x curl_z\boldsymbol{\tau}(x',y)\,\mathrm{d}x' - \frac{\partial g(y)}{\partial y}$$

Let's simplify our forcing and take the wind stress curl as zonally uniform, so that

$$\tau_T^y = 0, \quad \tau_T^x = -cos(\pi y) \tag{7.58}$$

so that the curl vanishes at $y = 0$ and $y = 1$ (Fig. 7.7). The curl in this case will be $curl_z\boldsymbol{\tau}_T = -\pi sin(\pi y)$. For this example, typical of subtropical latitudes, the wind stress is imparting a negative input of vorticity into the ocean everywhere.

The Sverdrup interior flow is

$$\psi_I(x,y) = \int_0^x curl_z\boldsymbol{\tau}(x',y)\mathrm{d}x' + g(y)$$
$$\psi_I(x,y) = \int_0^x \Big[-\pi sin(\pi y)\Big]\,\mathrm{d}x' + g(y)$$
$$\psi_I(x,y) = x\Big[-\pi sin(\pi y)\Big] + g(y)$$

We can define the arbitrary function of integration as $C(y) = -g(y)/curl_z\boldsymbol{\tau}_T$. So that our solution becomes

$$\psi_I(x,y) = x\Big[-\pi sin(\pi y)\Big] - \Big[C(y)curl_z\boldsymbol{\tau}_T\Big]$$
$$\psi_I(x,y) = x\Big[-\pi sin(\pi y)\Big] + C(y)\Big[\pi sin(\pi y)\Big]$$
$$\psi_I(x,y) = \pi\Big[C(y)-x\Big]sin(\pi y)$$

If C is a constant, then the zonal flow is $C\,curl_z\boldsymbol{\tau}$. Now, depending on C, we can either satisfy $\psi = 0$ at $x = 0$ or at $x = 1$

$$\psi_I(0,y) = \pi C\,sin(\pi y) = 0 \qquad \text{if} \quad C = 0 \tag{7.59}$$
$$\psi_I(1,y) = \pi(C-1)\,sin(\pi y) = 0 \quad \text{if} \quad C = 1 \tag{7.60}$$
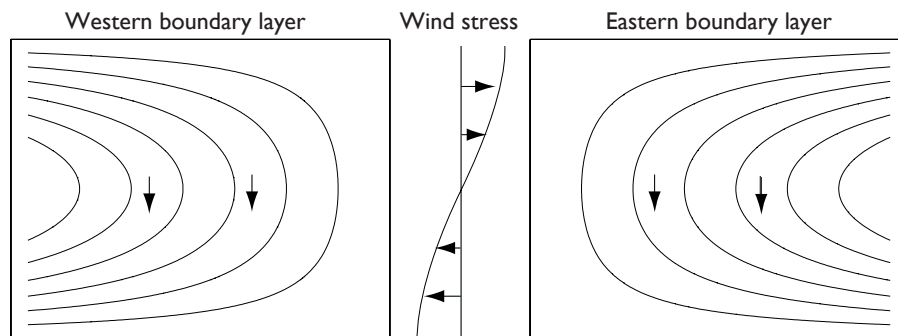
Figure 7.7: *Two possible Sverdrup flows, ψ_I, for the given wind stress. Each solution satisfies the no-flow condition at one boundary, either east or west. Both solutions have the same meridional interior flow. Which one is physically plausible? [from Vallis (2006)]*

We cannot satisfy both zonal boundary conditions of $\psi = 0$. And so a choice will have to be made on C, and more importantly on where the boundary layer will exist in order to satisfy the remaining boundary condition!

We could suppose the solution at the left of Fig.7.7, because the interior flow would go the same direction as the wind torque driving it. Friction should provide opposite torque in order to balance the angular momentum. An eastern boundary (solution at the right of Fig.7.7) would not be able to provide an anti-clockwise angular momentum (vorticity) capable of balancing vorticity input by the surface stress. Only the Western Boundary Current seems able to provide the required frictional force. We will expand on this 'vorticity argument' in Section 7.4

The boundary solution (asymptotic matching)

Let's now stretch the x-coordinate near the boundary, where $\phi(x,y)$ varies very rapidly in order to satisfy the boundary condition. The boundary could be at $x = 0$ or at $x = 1$:

$$x = \epsilon\alpha \quad \text{or} \quad x - 1 = \epsilon\alpha. \tag{7.61}$$

α is the stretched coordinate, having values $\mathcal{O}(1)$ in the boundary and ϵ is a small parameter. We now suppose that $\phi(\alpha, y)$ and using Eq.(7.55) write:

$$\partial_x(\psi_I + \phi) + \epsilon_s \nabla^2(\psi_I + \phi) = curl_z \boldsymbol{\tau}_T \qquad (7.62)$$

$$\partial_x \psi_I + \epsilon_s(\nabla^2 \psi_I + \nabla^2 \phi) + \frac{1}{\epsilon}\frac{\partial \phi}{\partial \alpha} = curl_z \boldsymbol{\tau}_T \qquad (7.63)$$

$$(7.64)$$

where $\nabla^2 \phi = \frac{1}{\epsilon^2}\frac{\partial^2 \phi}{\partial \alpha^2} + \frac{\partial^2 \phi}{\partial y^2}$. We know that ϕ_I satisfies Sverdrup balance, so the solution becomes

$$\epsilon_s(\nabla^2 \psi_I + \frac{1}{\epsilon^2}\frac{\partial^2 \phi}{\partial \alpha^2} + \frac{\partial^2 \phi}{\partial y^2}) + \frac{1}{\epsilon}\frac{\partial \phi}{\partial \alpha} = 0. \qquad (7.65)$$

We now make the simplest choice and choose $\epsilon = \epsilon_s$, so that the leading order balance is

$$\frac{\partial^2 \phi}{\partial \alpha^2} + \frac{\partial \phi}{\partial \alpha} = 0. \qquad (7.66)$$

The solution of which is $\phi = A(y) + B(y)e^{-\alpha}$.

The solution grows in the negative direction of α. But the solution cannot grow towards the interior or it would violate our assumption that ϕ is small in the interior. Hence, we impose $\alpha > 0$ and $A(y) = 0$. This implies the choice of $x = \epsilon\alpha$ so that $\alpha > 0$ for $x > 0$. The boundary layer is at $x = 0$: *a western boundary layer*, and it decays eastward for increasing α, towards the interior (Fig. 7.8).

We now choose $C = 1$, so that $\psi_I = 0$ at $x = 1$, and the solution for the given wind stress is

$$\psi_I = \pi(1 - x)\sin(\pi y) \qquad (7.67)$$

This satisfies the eastern boundary condition ($\psi = 0$ at $x = 1$).

$B(y)$ will now satisfy the other boundary condition in order to

$$\psi = \psi_I + \phi = 0 \quad \text{at} \quad x = 0. \qquad (7.68)$$

At $x = 0$:

$$\psi = \pi \sin(\pi y) + \phi = 0 \qquad (7.69)$$

Given that $\phi = B(y)e^{-\alpha}$, we have, at $x = 0$

$$\psi = \pi \sin(\pi y) + B(y) = 0, \qquad (7.70)$$

which readily implies that $B(y) = -\pi \sin(\pi y)$. The boundary layer correction is thus

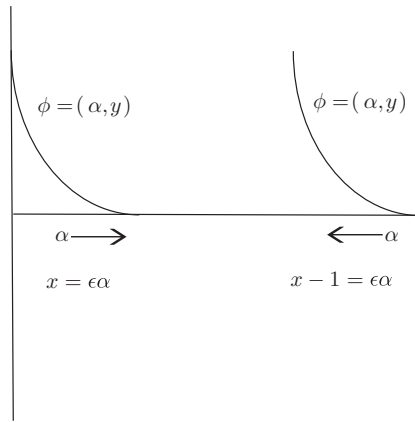$$\phi = -\pi \sin(\pi y)e^{-x/\epsilon_s}. \qquad (7.71)$$

Figure 7.8: *Two possible boundary solutions. Only the one on the western side decays towards the interior and satisfies the condition that $\phi = 0$ in the interior. The solution requires that $\alpha > 0$ and $x = \epsilon\alpha$.*

The boundary layer correction is thus proportional to the interior wind stress, as it has to balance that input of vorticity.

The full solution is thus

$$\psi = \psi_I + \phi \;=\; \pi\sin(\pi y) - x\pi\sin(\pi y) - \pi\sin(\pi y)e^{-x/\epsilon_s} \quad (7.72)$$

$$= \; \pi\sin(\pi y)\left(1 - x - e^{-x/\epsilon_s}\right). \quad (7.73)$$

The dimensional solution is (remember that $\psi = \hat{\psi}\frac{\tau_0}{\beta}; \tau = \hat{\tau}\tau_0; y = \hat{y}L; x = \hat{x}L$):

$$\boxed{\psi = \frac{\tau_0}{\beta}\pi\left(1 - \frac{x}{L} - e^{-x/(L\epsilon_s)}\right)\sin\frac{\pi y}{L}} \quad (7.74)$$

Given the chosen wind stress, this is a single gyre solution (Fig. 7.9), and for a realistic global wind stress the solution is shown in Fig. 7.11.

The boundary layer width

What is the width δ of the western boundary layer? In the interior, friction is small, and the balance is between wind stress and the β-effect:

$$|r\zeta| \ll |\beta v|. \quad (7.75)$$

With $r = \frac{f\delta}{H}$, this means that $\frac{f\delta}{HL} \ll \beta$. For friction to be small, we also have that

$$\epsilon_s = \frac{r}{L\beta} \ll 1 \quad \text{or} \quad \frac{r}{\beta} \ll L, \quad (7.76)$$
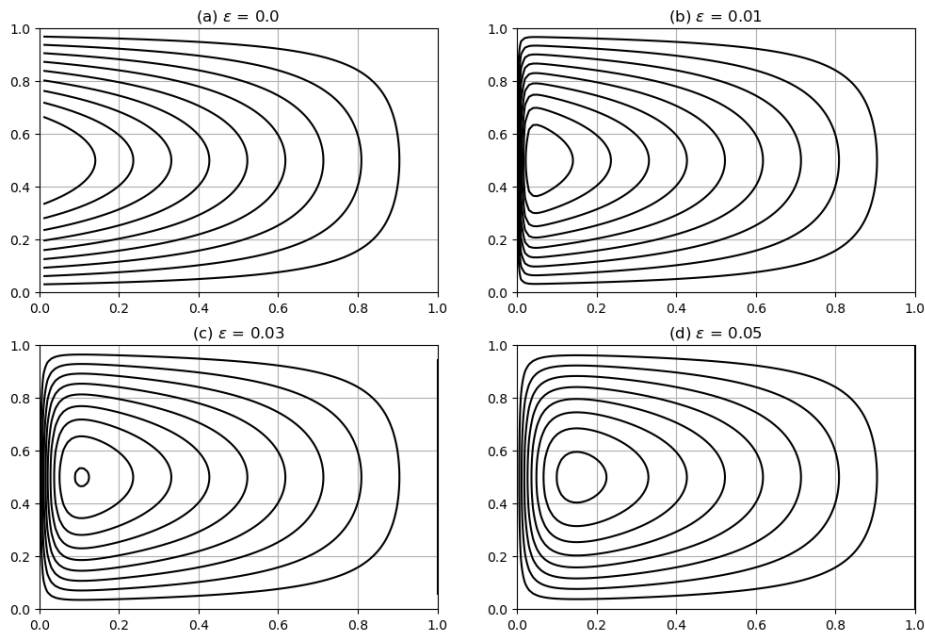
Figure 7.9: *Solutions of the Stommel model for a single-gyre wind-induced flow for different values of ε. Note that for ε=0 the model reduces to the Sverdrup balance.*
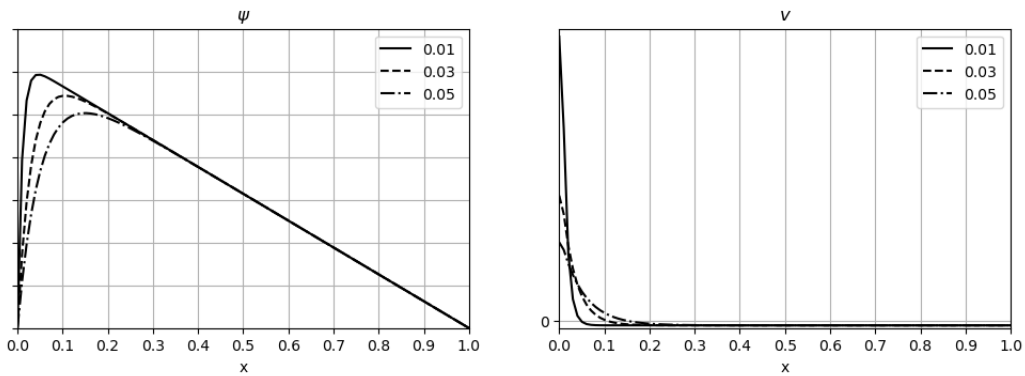

Figure 7.10: *Solutions of the Stommel model for a single-gyre wind-induced flow for different values of ε. Plotted are the streamfunction ψ and the meridional velocity $v = \partial\psi/\partial x$ at the centre of the gyre.*

where r measures bottom friction and L denotes the length scale of zonal variations of the geostrophic current.

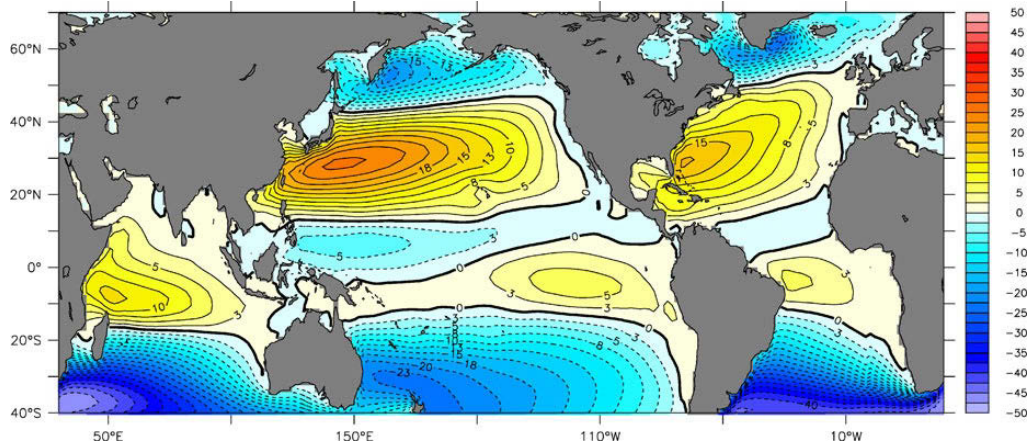However, when L becomes smaller, representing dynamics in the bound-

Figure 7.11: *Streamfunction ψ (in Sv) computed from the Stommel model with realistic wind stress curl and a boundary layer width δ = 100 km. [from Olbers et al. (2012)]*

ary layer, we have a different balance:

$$\frac{r}{\beta} \sim L, \tag{7.77}$$

and now $L = \mathcal{O}(\delta)$ so that the width of the Stommel boundary layer is

$$\boxed{\delta_S = \frac{r}{\beta}}. \tag{7.78}$$

Within this narrow boundary layer, $v_g > 0$ and $\bar{v} > 0$, balancing the interior Sverdrup flow. The total transport in the Sverdrup regime occurs between the eastern edge of the western boundary layer, $x = \delta_S$, and the eastern coast, $x = 1$. A corresponding transport must be compensated and returned within the boundary layer. This transport is thus prescribed by the wind outside the boundary layer, the Sverdrup regime. Because the boundary layer width is much smaller than the basin width, the currents in the boundary layer have to be much stronger than in the Sverdrup regime, as observed.

An f-plane solution

In the Stommel model, dissipation of vorticity arises from bottom frictional stresses within a bottom boundary layer.

In the case of a constant f, so that $\beta = \frac{\partial f}{\partial y} = 0$, the input of vorticity from the wind simply balances the opposing frictional dissipation everywhere. This leads to symmetric solutions, which are not realistic.

$$\underbrace{\beta \frac{\partial \psi}{\partial x}}_{\substack{0 \text{ for} \\ \text{the } f\text{-plane}}} = \underbrace{F_\tau(x,y)}_{\substack{\text{wind input} \\ \text{of vorticity}}} \qquad \underbrace{-r\nabla^2 \psi}_{\substack{\text{frictional dissipation} \\ \text{of vorticity}}} \qquad . \tag{7.79}$$

The vertical geostrophic velocity vanishes in the f-plane, and the two Ekman induced vertical velocities have to compensate each other. This is possible if

$$curl_z \widetilde{\boldsymbol{\tau}}_T = curl_z \widetilde{\boldsymbol{\tau}}_B = \frac{d}{2}\zeta_g \tag{7.80}$$

There is no boundary layer solution, and the balance is achieved everywhere within the basin (see Fig. 7.12).

If, conversely, $\beta \neq 0$, in the interior we find a balance between change in planetary vorticity and input of vorticity. In the narrow western boundary layer, the fluid column changes again its planetary vorticity but the source of vorticity is from frictional dissipation.

But given that the return flow was found on a western boundary layer, is bottom drag realistic?
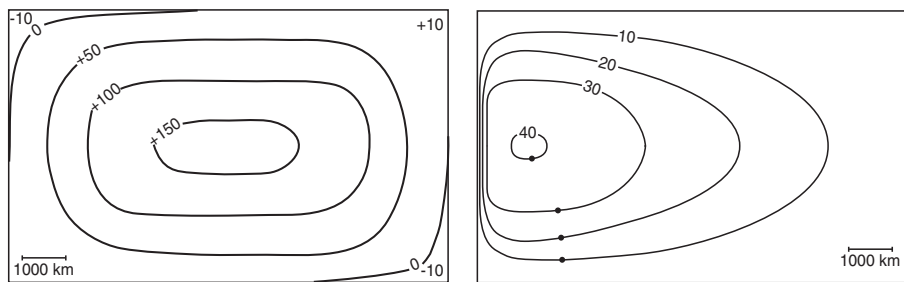

Figure 7.12: *Stommel's wind-driven circulation solution for a subtropical gyre with trades and westerlies. (a) Transport streamfunction ψ on a uniformly rotating Earth ($f = f_0$) and (b) westward intensification with the β-effect ($f = f_0 + \beta y$). [from Stommel (1948)]*

(a) no rotation

(b) Coriolis force constant

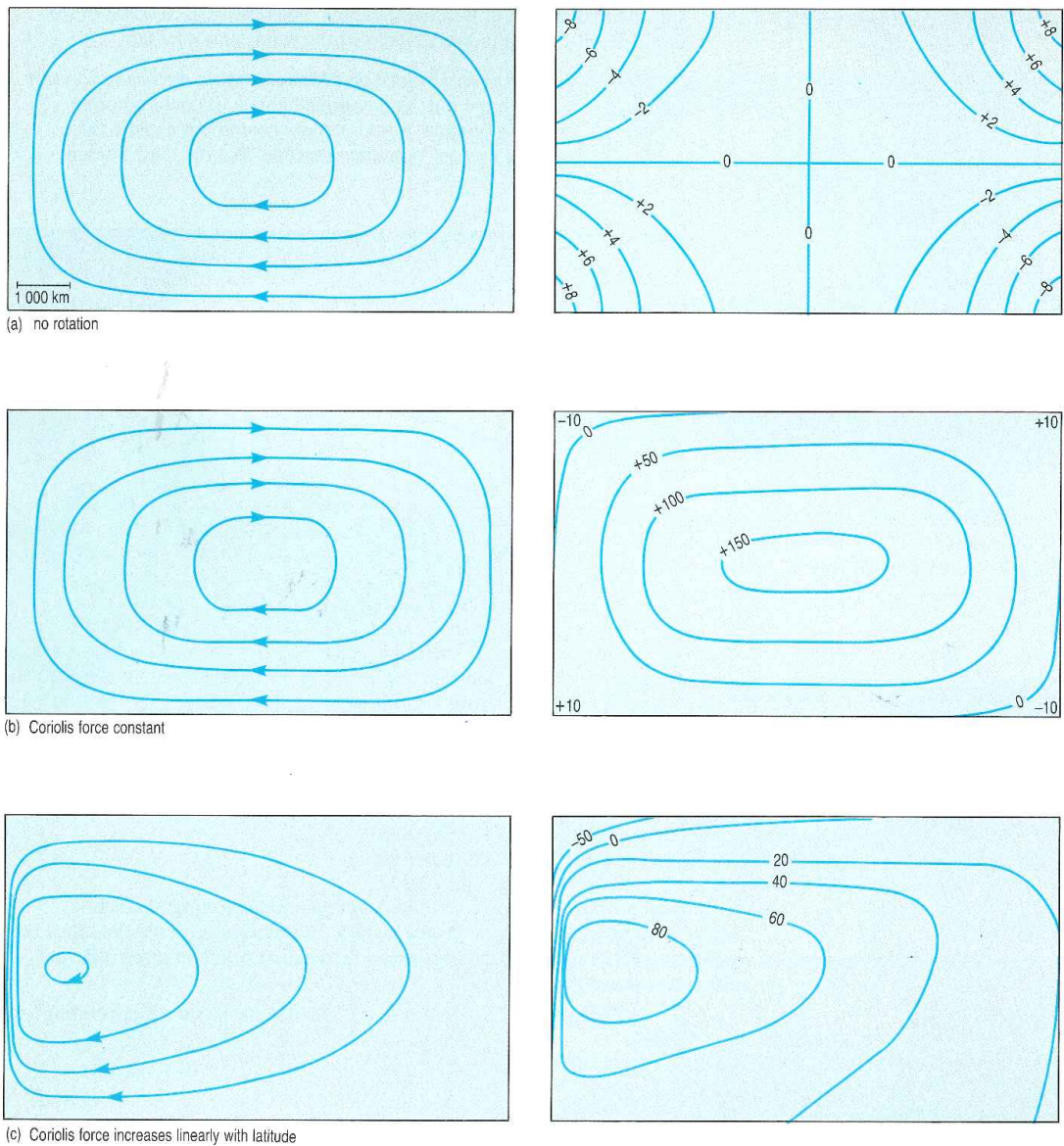(c) Coriolis force increases linearly with latitude

Figure 7.13: *(left panels) Streamfunction ψ and (right panels) sea-surface height η for a symmetrical gyral wind field (à la Stommel). In the case of no rotation f = 0 winds simply drive a symmetric circulation, just as you might expect from stirring a coffee cup. If f =const and β = 0 as in a flat Earth, there is again a symmetric solution with fluid rotating in geostrophic balance. Western intensification requires Earth to be a spinning sphere with planetary vorticity varying with latitude. [from Stommel (1948)]*

7.3   The Munk model

An Ekman bottom drag is not appropriate to balance the interior wind-driven circulation. This is because the circulation does not reach all the way down to the bottom and some other form/term is required to balance the interior transport. An extension of the Stommel problem was formulated by Munk, who introduced lateral harmonic viscosity.

Munk does not use a bottom drag and, given that the boundary layer is on a side, introduces horizontal viscosity. We can start from the set of primitive equations and our fluid is governed by

$$-fv = -\frac{\partial \phi}{\partial x} + \frac{\partial}{\partial x}\left(\frac{\nu_h}{\rho_0}\frac{\partial u}{\partial x}\right) + \frac{\partial}{\partial y}\left(\frac{\nu_h}{\rho_0}\frac{\partial u}{\partial y}\right) + \frac{\partial}{\partial z}\left(\frac{\nu_v}{\rho_0}\frac{\partial u}{\partial z}\right) \quad (7.81)$$

$$fu = -\frac{\partial \phi}{\partial y} + \frac{\partial}{\partial x}\left(\frac{\nu_h}{\rho_0}\frac{\partial v}{\partial x}\right) + \frac{\partial}{\partial y}\left(\frac{\nu_h}{\rho_0}\frac{\partial v}{\partial y}\right) + \frac{\partial}{\partial z}\left(\frac{\nu_v}{\rho_0}\frac{\partial v}{\partial z}\right) \quad (7.82)$$

$$0 = \frac{\partial u}{\partial x} + \frac{\partial v}{\partial y} + \frac{\partial w}{\partial z} \quad (7.83)$$

or in a simpler form

$$\mathbf{f} \times \mathbf{u} = -\nabla \phi + \frac{1}{\rho_0} \nabla \cdot (\nu \nabla \mathbf{u}) \quad (7.84)$$

$$\nabla_3 \cdot \mathbf{u} = 0 \quad (7.85)$$

which are very similar to the set of equations used by Stommel (Eq. 7.21), but now we have introduced a term related to horizontal turbulent viscosity. These will be the key to introduce a frictional dissipation similar to the Stommel bottom drag.

Again, assume a vertically-integrated ocean, let's vertically integrate and pose:

$$\Phi = \int_{-H}^{z} \phi \, dz; \quad \overline{u} = \int_{-H}^{z} \rho_0 u \, dz; \quad \overline{v} = \int_{-H}^{z} \rho_0 v \, dz \quad (7.86)$$

we find

$$-f\overline{v} = -\frac{\partial \Phi}{\partial x} + \nu_h \nabla^2 \overline{u} + \int_{-H}^{z} \frac{\partial}{\partial z} \nu_v \frac{\partial u}{\partial z} \, dz \quad (7.87)$$

$$f\overline{u} = -\frac{\partial \Phi}{\partial y} + \nu_h \nabla^2 \overline{v} + \int_{-H}^{z} \frac{\partial}{\partial z} \nu_v \frac{\partial v}{\partial z} \, dz \quad (7.88)$$

$$0 = \frac{\partial \overline{u}}{\partial x} + \frac{\partial \overline{v}}{\partial y} \quad (7.89)$$

We have set $w = 0$ at $z = 0$ and $z = -H$, and note that the stress tensor was defined as

$$\tau^x = \left(\nu_v \frac{\partial u}{\partial z}\right)_{z=0} - \left(\nu_v \frac{\partial u}{\partial z}\right)_{z=-H} \tag{7.90}$$

$$\tau^y = \left(\nu_v \frac{\partial v}{\partial z}\right)_{z=0} - \left(\nu_v \frac{\partial v}{\partial z}\right)_{z=-H}. \tag{7.91}$$

Ignoring bottom contributions this yields

$$-f\overline{v} = -\frac{\partial \Phi}{\partial x} + \nu_h \nabla^2 \overline{u} + \tau_T^x \tag{7.92}$$

$$f\overline{u} = -\frac{\partial \Phi}{\partial y} + \nu_h \nabla^2 \overline{v} + \tau_T^y \tag{7.93}$$

$$0 = \frac{\partial \overline{u}}{\partial x} + \frac{\partial \overline{v}}{\partial y}. \tag{7.94}$$

Now, as usual, take the curl of the horizontal momentum equations and use a streamfunction for the non-divergent flow to obtain:

$$\boxed{\beta \frac{\partial \psi}{\partial x} = curl_z \boldsymbol{\tau}_T + \nu_h \nabla^4 \psi} \tag{7.95}$$

The operator $\nu_h \nabla^4$ parameterizes viscosity as a biharmonic turbulent viscosity. This simple model captures a western boundary 'return' current and an interior Sverdrup flow. The simple model points to the role of the wind stress curl, and not the wind *per se*. The strength of the return current is dictated by dynamics outside of the boundary layer itself, i.e. the interior wind stress curl. This explains why some boundary currents (the Gulf Stream) are stronger than others (the Brazil current), which are driven by weaker wind stress curl (Fig. 7.14).
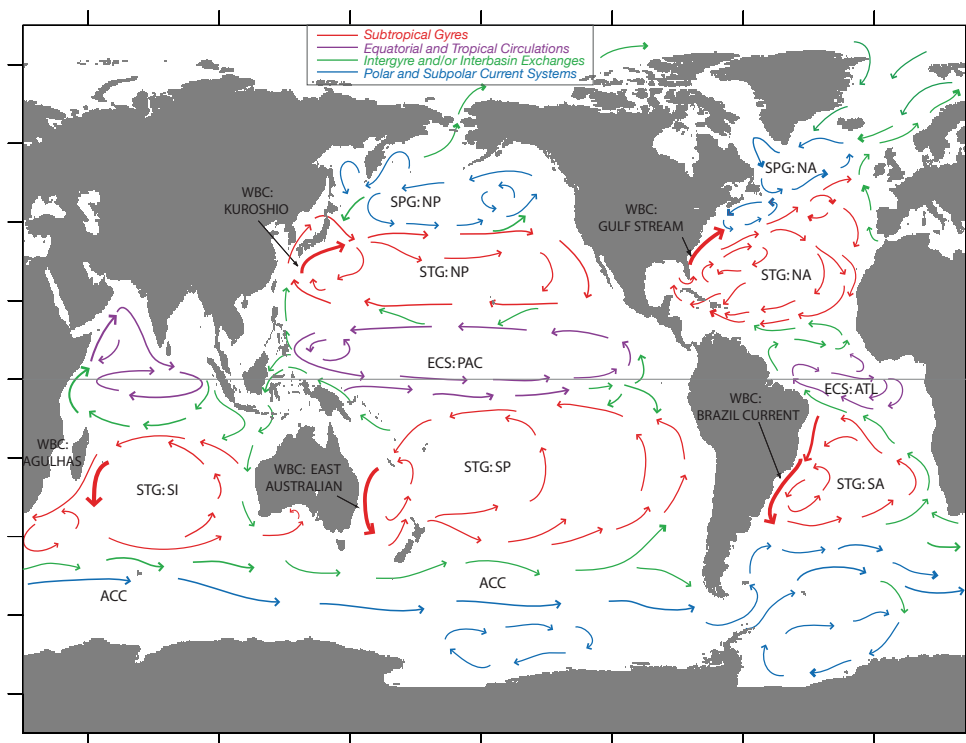
Figure 7.14: *A schema of the main currents of the global ocean [from Vallis (2006)].*

7.3.1 Interior and boundary solutions

The vorticity equation now reads

$$\beta \frac{\partial \psi}{\partial x} = curl_z \boldsymbol{\tau}_T + \nu_h \nabla^2 \zeta = curl_z \boldsymbol{\tau}_T + \nu_h \nabla^4 \psi. \qquad (7.96)$$

This is the so-called MUNK MODEL. We need two boundary conditions at each wall because of the higher-order term. One is $\psi = 0$ to satisfy no-normal flow condition. The second boundary condition could be:

1. Zero vorticity ($\zeta = 0$). Since $\psi = 0$ along the boundary, this is equivalent to $\frac{\partial^2 \psi}{\partial n^2} = 0$, where $\frac{\partial}{\partial n}$ denotes a derivative normal to the boundary. At $x = 0$, this condition becomes $\frac{\partial v}{\partial x} = 0$: there is no horizontal shear at the boundary. This is called a *'free-slip'* condition.

2. No flow along the boundary. This is equivalent to $\frac{\partial \psi}{\partial n} = 0$. At $x = 0$, this condition becomes $v = 0$. This is called a *'no-slip'* condition.

Either could be used, and we will solve the *'no-slip'* problem. If we use the same wind stress

$$\tau^x = -cos(\pi y / L), \qquad (7.97)$$

and non-dimensionalize (7.96) in a similar way to the Stommel problem

$$\frac{\partial \hat{\psi}}{\partial \hat{x}} - \epsilon_M \nabla^4 \hat{\psi} = curl_z \widetilde{\boldsymbol{\tau}}_T. \qquad (7.98)$$

Here $\epsilon_M = \nu / (\beta L^3)$. Again, the full solution will be the contribution of a western boundary layer correction and an interior Sverdrup flow

$$\hat{\psi} = \psi_I + \phi(\alpha, y). \qquad (7.99)$$

The Munk problem does become

$$-\epsilon_M \left(\nabla^4 \psi_I + \frac{1}{\epsilon^4} \frac{\partial^4 \phi}{\partial \alpha^4} \right) + \frac{1}{\epsilon} \frac{\partial \phi}{\partial \alpha} = 0. \qquad (7.100)$$

Of which the leading order balance is

$$-\frac{\partial^4 \phi}{\partial \alpha^4} + \frac{\partial \phi}{\partial \alpha} = 0. \qquad (7.101)$$

Subject to suitable boundary conditions and the interior Sverdrup solution

$$\psi_I = \pi (1 - x) sin(\pi y), \qquad (7.102)$$

where we have taken $C = 1$ as in Eq.(7.60) of the Stommel problem, the solution to the Munk problem is (a non-trivial algebraic exercise ...):

$$\hat{\psi} = \pi \sin(\pi\hat{y})\left\{1 - \hat{x} - e^{-\hat{x}/(2\epsilon)}\left[\cos\left(\frac{\sqrt{3}\hat{x}}{2\epsilon}\right) + \frac{1 - 2\epsilon}{\sqrt{3}}\sin\left(\frac{\sqrt{3}\hat{x}}{2\epsilon}\right)\right] + \epsilon e^{(\hat{x}-1)/\epsilon}\right\}.$$

(7.103)

The solution, for different values of ϵ, is shown in Fig. 7.15.

The Munk viscous boundary layer brings the tangential and the normal velocity to zero (Fig. 7.16).

The boundary layer width

What is the thickness of the Munk boundary layer? We have the following balance

$$\beta\frac{\partial\psi}{\partial x} \sim \nu\nabla^4\psi$$

(7.104)

$$\beta\frac{U}{L^2} \sim \nu\frac{U}{L^5}$$

(7.105)

$$\beta \sim \frac{\nu}{L^3},$$

(7.106)

in the boundary layer lateral diffusion of momentum will be important and will extract momentum imparted by the wind stress. If lateral viscosity is important, the length scale will be $L = \mathcal{O}(\delta)$, and so the boundary layer width is given by

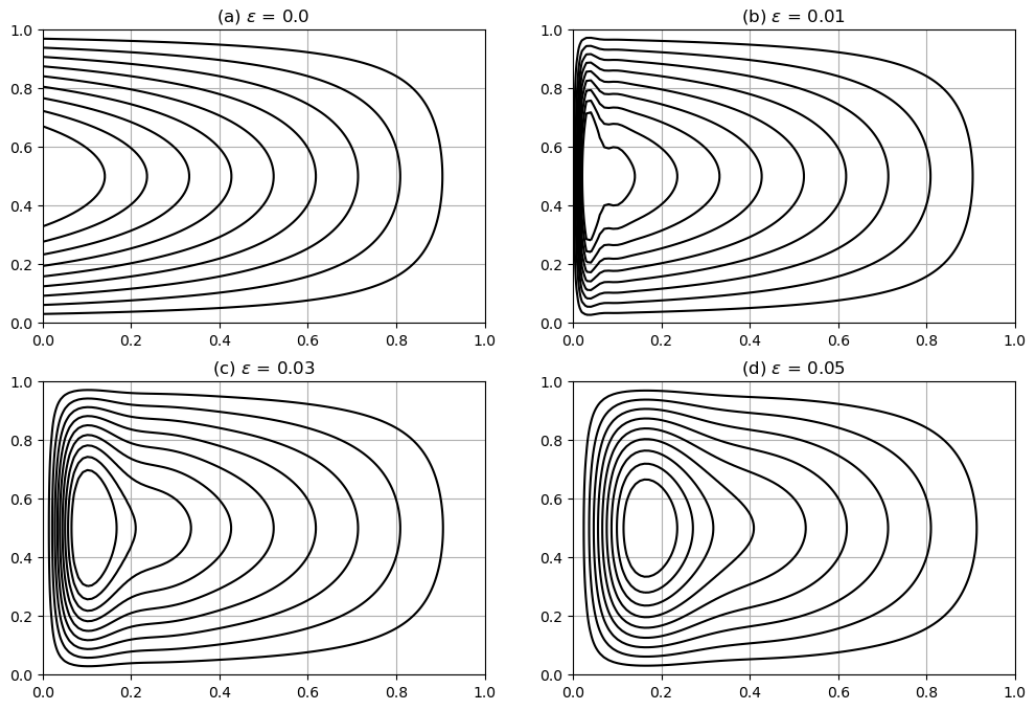$$\boxed{\delta_M \sim \left(\frac{\nu}{\beta}\right)^{1/3}}$$

(7.107)

Figure 7.15: *Solutions of the Munk model for a single-gyre wind-induced flow for different values of ϵ. Note that for ϵ=0 the model reduces to the Sverdrup balance.*
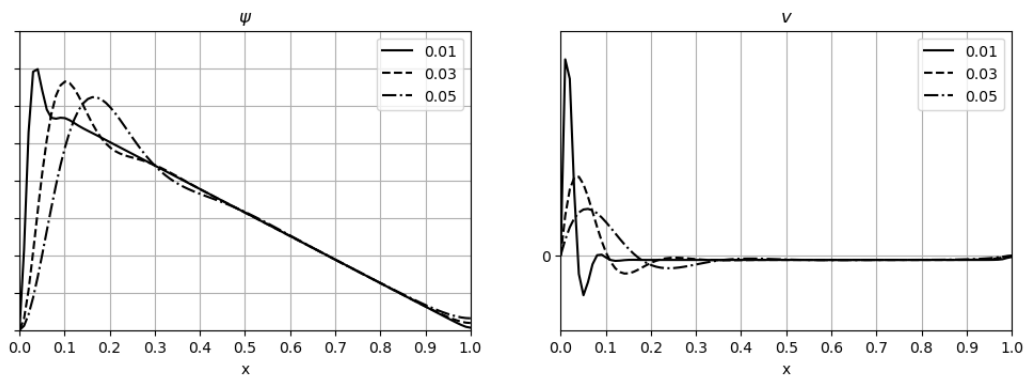

Figure 7.16: *Solutions of the Munk model for a single-gyre wind-induced flow for different values of ϵ. Plotted are the streamfunction ψ and the meridional velocity $v = \partial\psi/\partial x$ at the centre of the gyre. Note that the Munk model brings the velocity v to zero at the western boundary.*

Figure 7.17: *Franklin wondered why journeys towards the east were faster than return trips on his voyages across the Atlantic Ocean between the Colonies and Europe. His curiosity led him to be the first to chart the Gulf Stream on 1786. Franklin was talking to his cousin, Timothy Folger, who was the captain of a merchant ship. He asked why it took ships like Folger's so much less time to reach America than it took official mail ships. It struck Folger that the British mail captains must not know about the Gulf Stream, with which he had become well-acquainted in his earlier years as a Nantucket whaler. Folger told Franklin that whalers knew about the "warm, strong current" and used it to help their ships track and kill whales. But the mail ships "were too wise to be counselled by simple American fishermen" and kept sailing against the current, losing time as they did so.*
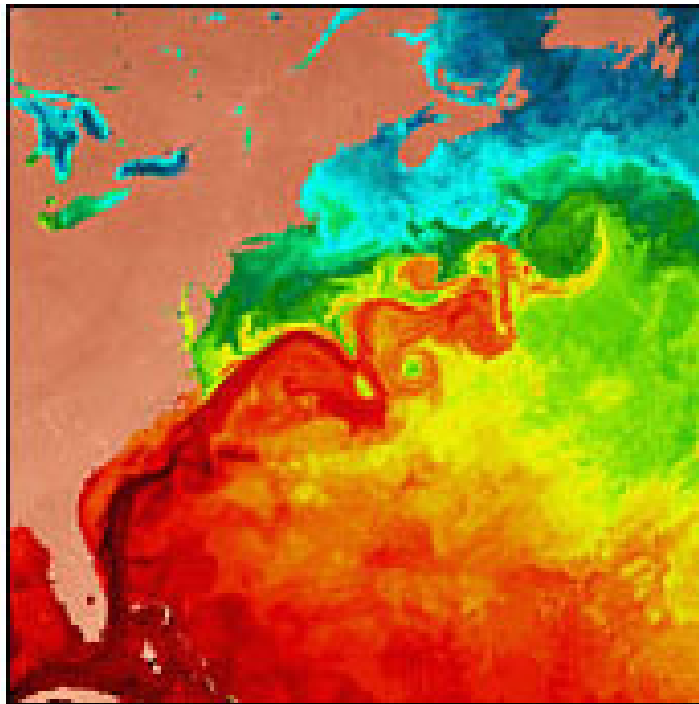
Figure 7.18: *A satellite image of the Gulf Stream.*

Neither the Stommel nor the Munk model are accurate representations of the real ocean. We need to include non-linearities and topographic effects to improve our solution.

The non-linear Stommel-Munk problem is

$$\frac{\partial \zeta}{\partial t} + J(\psi, \zeta) + \beta \frac{\partial \psi}{\partial x} = curl_z \boldsymbol{\tau}_T - r\nabla^2 \psi + \nu \nabla^2 \zeta. \tag{7.108}$$

And the steady non-linear Stommel-Munk problem is

$$J(\psi, \zeta) + \beta \frac{\partial \psi}{\partial x} = curl_z \boldsymbol{\tau}_T - r\nabla^2 \psi + \nu \nabla^2 \zeta. \tag{7.109}$$

The need for friction

Consider the steady barotropic flow

$$\frac{D\,(f + \zeta)}{D\,t} = F \qquad\qquad (7.110)$$

satisfying

$$\boxed{\boldsymbol{u} \cdot \nabla q = curl_z \boldsymbol{\tau}_T + \text{Friction}}, \qquad\qquad (7.111)$$

where $q = \nabla^2 \psi + \beta y$ and the last term on the rhs represents frictional effects. $\boldsymbol{u}$ is divergent-free and we can integrate the lhs over some area A between two closed streamlines, ψ_1 and ψ_2. Using the divergence theorem[2] :

$$\int_A \nabla \cdot (\boldsymbol{u} q)\, dA = \oint_{\psi_1} \boldsymbol{u} q \cdot \boldsymbol{n}\, dl - \oint_{\psi_2} \boldsymbol{u} q \cdot \boldsymbol{n}\, dl = 0. \qquad\qquad (7.112)$$

Here $\boldsymbol{n}$ is the unit vector normal to the streamline so that $\boldsymbol{u} \cdot \boldsymbol{n} = 0$. The integral of the wind-stress curl over the area A will not be zero. This means that a balance between wind-stress curl and friction can only be achieved if every closed contour passes through a region where frictional effects are non-zero, and are important somewhere along the streamline path.

Thus, in the Stommel and Munk models, every streamline must pass through the frictional western boundary layer.

---

[2]Here we use the 2D divergence theorem for a vector field $F(x,y)$: $\iint_A \text{div}\, F\, dA = \oint_{\partial A} F \cdot \boldsymbol{n}\, dl$

7.4 Westward intensification

PV balance interpretation

How does the potential vorticity balance work in Munk's model (which is combined with Sverdrup's model)?

Why do we find the boundary current on the western side rather than the eastern side, or even within the middle of the basin (if considering Stommel's bottom friction)?

In the Sverdrup interior of a subtropical gyre, when the wind causes Ekman pumping, the water columns are squashed, they move equatorward to lower planetary vorticity.

To return to a higher latitude, there must be forcing that puts the higher vorticity back into the fluid. This cannot be in the form of planetary vorticity, since this is already contained in the Sverdrup balance. Therefore, the input of vorticity must affect the relative vorticity.

Consider a western boundary current for a Northern Hemisphere subtropical gyre, with friction between the current and the side wall (Munk's model). The effect of the side wall is to reduce the boundary current velocity to zero at the wall. Therefore, the boundary current has positive relative vorticity. This vorticity is injected into the fluid by the friction at the wall, and allows the current to move northward to higher Coriolis parameter f.

On the other hand, if the narrow jet returning flow to the north were on the eastern boundary, the side wall friction would inject negative relative vorticity, which would make it even more difficult for the boundary current fluid to join the interior flow smoothly.

Therefore, vorticity arguments require that frictional boundary currents be on the western boundary. You can go through this exercise for subpolar gyres as well as for both types of gyres in the Southern Hemisphere and will find that a western boundary current is required in all cases!
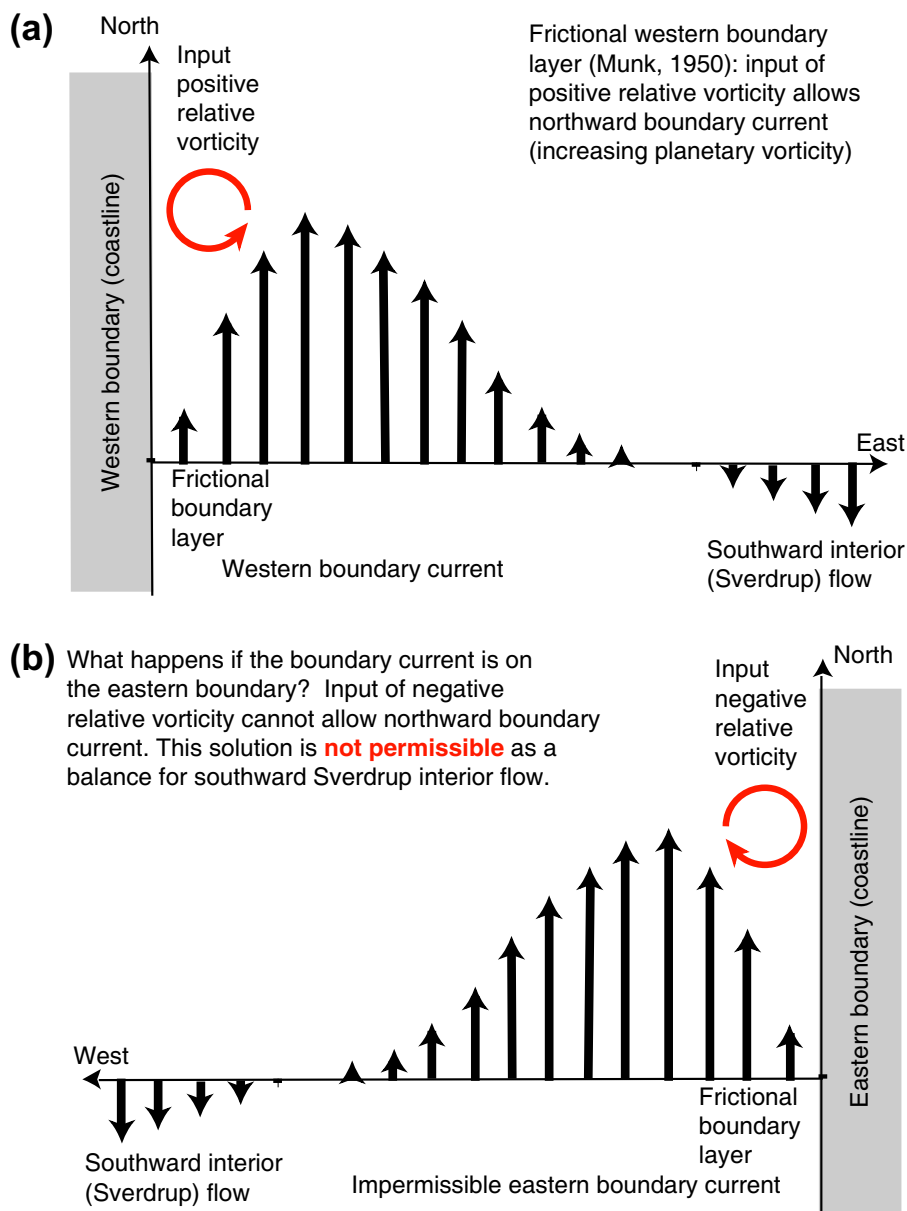
(a) North

Input positive relative vorticity

Frictional western boundary layer (Munk, 1950): input of positive relative vorticity allows northward boundary current (increasing planetary vorticity)

Western boundary (coastline)

East

Frictional boundary layer

Western boundary current

Southward interior (Sverdrup) flow

(b) What happens if the boundary current is on the eastern boundary? Input of negative relative vorticity cannot allow northward boundary current. This solution is **not permissible** as a balance for southward Sverdrup interior flow.

North

Input negative relative vorticity

Eastern boundary (coastline)

West

Southward interior (Sverdrup) flow

Frictional boundary layer

Impermissible eastern boundary current

Figure 7.19: *(a) Vorticity balance at a western boundary, with side wall friction (Munk's model). (b) Hypothetical eastern boundary vorticity balance, showing that only western boundaries can input the positive relative vorticity required for the flow to move northward. [from Talley et al. (2011)]*

Western intensification understood as westward drift

Here we'll give a slightly different explanation of why the boundary current is in the west. It is not really a different explanation, because the cause is still **differential rotation**, but we'll think about it quite differently. We'll see the effect of differential rotation is to make patterns propagate to the west, and hence the response to the wind's forcing piles up in the west and produces a boundary current there.
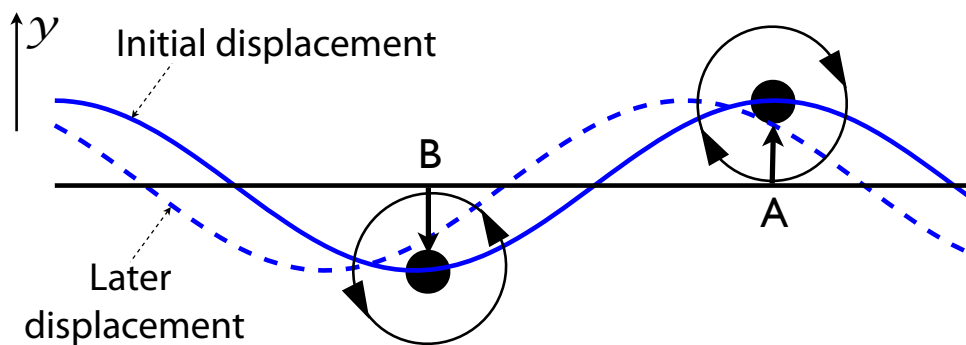

Figure 7.20: *If parcel A is displaced northwards then its clockwise spin increases, causing the northwards displacement of parcels that are to the west of A. A similar phenomena occurs if parcel B is displaced south. Thus, the initial pattern of displacement propagates westward. [from Vallis (2006)]*

Let's now imagine a line of parcels (Fig. 7.20). Suppose we displace parcel 'A' northwards. Because the Earth's spin is anti-clockwise (looking down on the North Pole) and this increases as the parcel moves northward, then the parcel must spin more in a clockwise direction in order to preserve its total vorticity

$$q = f + \zeta. \tag{7.113}$$

This spin will have the effect of moving the fluid that is just to west of the original parcel northwards, and then this will spin more clockwise, moving the fluid to its left northwards, and so on. The northwards displacement thus propagates *westward*, whereas parcels to the east of the original displacement are returned to their original position so that there is no systematic propagation to the east. Similarly, a parcel that is displaced southwards (parcel B) also causes the pattern to move westwards. We have just described the westward propagation of a simple *Rossby wave*, but the same effect occurs with more complex patterns and in particular, with the gyre as a whole.

Thus, imagine that an east-west symmetric gyre is set up, with the winds and friction in equilibrium, as in an f-plane. Differential rotation then tries to move the pattern westward, but of course the entire pattern cannot move to the west because there is a coastline in the way! The gyre thus squashes up against the western boundary creating an intense western boundary current.

This way of viewing the matter serves to emphasize that **it is not frictional effects that cause western intensification; rather, frictional effects allow the flow to come into equilibrium with an intense western boundary current, with the ultimate cause being the westward propagation due to differential rotation.**

In fact, the location of the boundary layer, on the west, does not depend on the sign of the wind-stress curl (the sign is reversed in a subpolar gyre and the flow is southward within a western boundary current) nor on the sign of the Coriolis parameter (think about what happens in the southern hemisphere where $f < 0$). The western location depends on β, which is always positive (Fig. **??**).

The Stommel & Munk models of the Wind-Driven Circulation

– The Model

1. The model uses the vertically integrated planetary-geostrophic equations (or a homogeneous fluid) with nonlinearities neglected.

2. The model uses a flat bottomed ocean.

3. • In the Stommel model, bottom friction is parameterized by a *linear drag*.

   • In the Munk model, lateral friction is parameterized by a *Newtonian harmonic viscosity* .

– Solution

1. The transport in the Sverdrup interior is equatorwards for an anti-cyclonic wind-stress-curl.

2. The Sverdrup transport is exactly balanced by a poleward transport in a westward boundary layer.

3. The boundary layer satisfies mass conservation, and must be a *western* boundary layer for friction to provide a force of opposite sign as the motion in the interior.

   The boundary layer is a *frictional boundary layer*.

4. The western location does not depend on the sign of the Coriolis parameter nor on the sign of the wind stress. The location does depend on the sign of β.

5. • In the Stommel model the balance in the western boundary layer is between $r\nabla^2\psi$ and $\beta\frac{\partial\psi}{\partial x}$. The boundary layer width is $\delta_S = \left(\frac{r}{\beta}\right)$. If r, the inverse frictional time, is 1/20 days^{-1}, then $\delta_S \approx$ 60 km.

   • In the Munk model the balance in the western boundary layer is between $\nu\nabla^4\psi$ and $\beta\frac{\partial\psi}{\partial x}$. The boundary layer width is $\delta_M = \left(\frac{\nu}{\beta}\right)^{1/3}$.

7.5 Topographic effects on western boundary currents

We have so far assumed a flat ocean bottom in order to derive the equations of the Sverdrup, Stommel and Munk models. This allowed us to eliminate the depth-integrated pressure gradient force when taking the curl of the depth-integrated momentum budget. But the ocean is certianly not flat, and sloping sidewalls will actually change the behaviour of western boundary currents. They can even become inviscid if the flow is preserving its potential vorticity by flowing along f/h contours. If the ocean is flat, then a meridional flow within a boundary layer exists thanks to frictional effects permitting the flow to cross f contours. If sidewalls are sloping then the flow can move quasi-northward (along f/h contours) preserving its potential vorticity.

7.5.1 Bottom pressure stress

We now consider the effects of topography and stratification on the circulation of a wind-driven gyre. Interactions of pressure with a variable topography can generate a meridional flow. The vorticity balance of a depth-integrated flow now possesses and extra term describing the influence of topography on the flow.

Let's define $h = h(x, y)$ and let's consider a stratified ocean in which density is not a constant. The momentum equation in planetary-geostrophic approximation is

$$f \times u = -\nabla\phi + F \tag{7.114}$$

where F represents both frictional and wind forcing terms. Integrating this over the entire depth of the water column

$$f \times \overline{u} = -\int_{\eta_B}^{0} \nabla\phi \, \mathrm{d}z + \overline{F} \tag{7.115}$$

where $\overline{x} = \int_{\eta_B}^{0} x \, \mathrm{d}z$. Now remember the Leibnitz rule:

$$\nabla \int_{\eta_B}^{0} \phi \, \mathrm{d}z = \int_{\eta_B}^{0} \nabla\phi \, \mathrm{d}z + \phi_0 \nabla\eta_T - \phi_B \nabla\eta_B, \tag{7.116}$$

where the second term on the rhs vanishes given that $\eta_T = z = 0$ at the top. For our purpose:

$$\int_{\eta_B}^{0} \nabla \phi \, dz = \nabla \int_{\eta_B}^{0} \phi \, dz + \phi_B \nabla \eta_B, \tag{7.117}$$

and so we write the vertically integrated momentum equations as

$$f \times \overline{u} = -\nabla \int_{\eta_B}^{0} \phi \, dz - \phi_B \nabla \eta_B + \overline{F}. \tag{7.118}$$

The second term on the rhs is the stress in the fluid due to the correlation between pressure gradient and topography. It is called bottom *form drag*.

If we rewrite the vertical integral of the pressure:

$$\int_{-h}^{0} \phi \, dz = (\phi z)|_{-h}^{0} - \int_{-h}^{0} z(\partial \phi / \partial z) dz = \phi_B h + \int_{-h}^{0} z \rho g \, dz = \phi_B h + E, \tag{7.119}$$

where we have used hydrostasy $\partial \phi / \partial z = -\rho g$ and defined the vertically-integrated potential energy $E = g \int_{-h}^{0} z \rho \, dz$.

Our vertically integrated momentum thus become

$$f \times \overline{u} = -\nabla \int_{\eta_B}^{0} \phi \, dz - \phi_B \nabla \eta_B + \overline{F} \tag{7.120}$$

$$= -\nabla \int_{\eta_B}^{0} \phi \, dz + \phi_B \nabla h + \overline{F} \tag{7.121}$$

$$= -\nabla \left(\phi_B h + E \right) + \phi_B \nabla h + \overline{F} \tag{7.122}$$

$$= -h \nabla \phi_B - \nabla E + \overline{F}. \tag{7.123}$$

Where we have used $\nabla \eta_B = -\nabla h$, taking the top of the ocean at $z = 0$ and h the fluid column. To obtain a vorticity balance equation, and eliminating the pressure terms, we divide by h and take the curl. After using the streamfunction $(u, v) = (-\partial \psi / \partial y, \partial \psi / \partial x)$:

$$\boxed{J\left(\psi, f/h\right) + J\left(h^{-1}, E\right) = curl_z(\overline{F}/h)} \tag{7.124}$$

Assuming a flat bottom and constant density, we see that a torque provided by the wind stress balances the torque introduced by bottom friction and a torque related to the change in planetary vorticity, just as in Stommel. However, now an extra term appears which is related to the combined effect of stratification and topographic variations (or Joint Effect of Baroclinicity And Relief - JEBAR - term): $J\left(h^{-1}, E\right)$. For a constant h, the JEBAR term vanishes and we recover the Stommel problem

$$\beta \frac{\partial \psi}{\partial x} = curl_z \overline{F} \tag{7.125}$$

An alternative derivation accounting for the effect of topography and stratification is given by eliminating the potential energy term instead of the bottom pressure term. Going back to

$$f \times \overline{u} = -\nabla \int_{\eta_B}^{0} \phi \, dz - \phi_B \nabla \eta_B + \overline{F} \tag{7.126}$$

and taking the curl gives[3]

$$\beta \overline{v} = curl_z \overline{F} - curl_z(\phi_B \nabla \eta_B) = curl_z \overline{F} - J\left(\phi_B, \eta_B\right). \tag{7.127}$$

The last term on the rhs is the bottom pressure-stress curl, or form-drag curl, or bottom pressure torque. And now this equation holds for both a homogeneous and stratified fluid.

For a homogeneous, frictionless and unforced gyre, this reduces to

$$\boxed{\beta \overline{v} = -J\left(\phi_B, \eta_B\right)} \tag{7.128}$$

or

$$\beta \overline{v} = -\nabla \phi_B \times \nabla \eta_B \tag{7.129}$$

There can be a meridional flow only if pressure gradient has a component parallel to topographic contour (the isobars are not aligned with topographic contours), and the term on the rhs is non-zero. The meridional flow is driven by the curl of the form drag. In a flat-bottomed ocean, the form drag is zero, and the meridional flow must be forced or viscous.

---

[3]$curl_z(h\nabla \phi_B) = curl_z(\phi_B \nabla \eta_B)$

f/h **contours**

If we consider an ocean where both forcing and friction are absent, and assuming an homogeneous gyre, the vorticity balance simplifies to

$$J\left(\psi, f/h\right) = 0 \qquad (7.130)$$

In an inviscid, unforced, and unstratified flow, ψ is a function of f/h, and streamlines of constant ψ and (f/h) contours coincide. In this case, the depth-integrated large-scale flow must follow f/h contours. The f/h contours form the characteristics of the differential equation above. This is called a *free mode*, driven solely by the bottom pressure-stress curl.

This is a statement about the balance between the vortex stretching by changes in topography and change in planetary vorticity of the fluid column. Consider a sloping sidewall, if a water column moves down the slope it will stretch in the vertical and increase its vorticity $(f + \zeta)$. On a
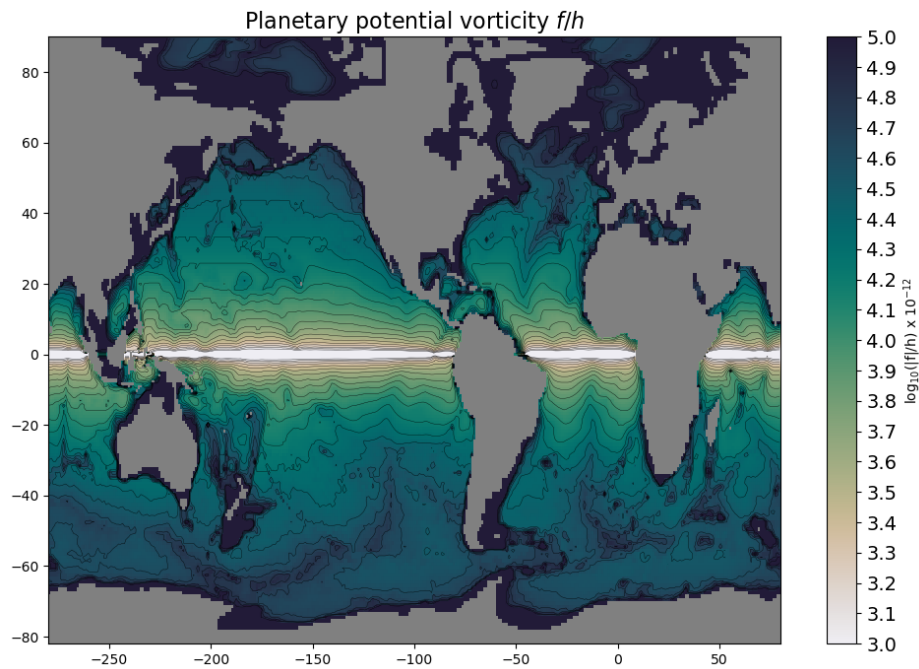
Figure 7.21: *Contours of planetary potential vorticity, f/h. Shown is $log_{10}(|f|/h\,[10^{-12}\,m^{-1}s^{-1}])$. For constant h, the f/h contours would follow latitude circles. The influence of topography on the depth-averaged flow is small in the tropics but becomes large at higher latitudes. In the Atlantic Ocean, the imprint of the mid-Atlantic ridge can be seen in the region of the subtropical gyres.*
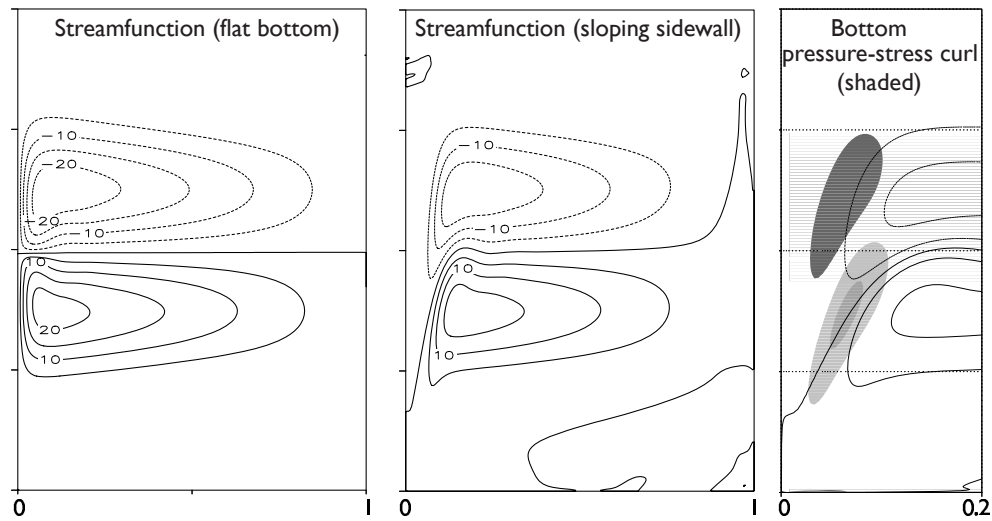
Figure 7.22: *Numerical results for a homogeneous problem, flat bottom domain and a domain with sloping western sidewall. The shaded regions in the right panels show the regions where bottom pressure-stress curl is important in the meridional flow of the western boundary current. [from Vallis (2006)]*

basin scale this will be balanced by changes in f rather than changes in ζ, so the PV balance reduces to $q = f/h$. In order to conserve PV, the column will be displaced meridionally, moving along f/h contours. The new f will be modulated by the thickness change h_2/h_1. For a constant h, f/h contours would follow latitude circles.

This vorticity conservation principle is shown by the linear vorticity equation:

$$\beta v = f\frac{\partial w}{\partial z} + \frac{\partial}{\partial z}\left(\tau_x^y - \tau_y^x\right) \tag{7.131}$$

Now, integrating vertically the vertical velocity does not vanish (assuming that $w_T = 0$):

$$\underbrace{\beta\overline{v}}_{\substack{\text{change in} \\ \text{planetary vorticity}}} = \underbrace{curl_z\boldsymbol{\tau}_T}_{\substack{\text{torque by} \\ \text{the wind}}} - \underbrace{curl_z\boldsymbol{\tau}_B}_{\substack{\text{torque by} \\ \text{bottom friction}}} - \underbrace{fw_B}_{\substack{\text{stretching of} \\ \text{water column}}} \tag{7.132}$$

Now that this is clear, we can go back to the vertically integrated vorticity balance

$$\beta\overline{v} = curl_z\overline{F} - curl_z(\phi_B\nabla\eta_B), \tag{7.133}$$

and considering both surface forcing and bottom drag we have the follow-

ing vorticity budget for the vertically integrated flow

$$\underbrace{\beta\overline{v}}_{1} = \underbrace{curl_z\overline{\tau}_T}_{2} - \underbrace{curl_z\overline{\tau}_B}_{3} - \underbrace{curl_z(\phi_B\nabla\eta_B)}_{4}. \qquad (7.134)$$

(1)+(2) is the Sverdrup balance; (1)+(2)+(3) is the Stommel problem. (4) introduces the bottom pressure torque.

The torque by the wind stress drives a meridional flow across f-lines (Fig. 7.23), as in Sverdrup balance. The western boundary layer is then dominated by a balance between the meridional flow (βv) and the bottom pressure-stress curl. Only where the flow crosses f/h contours is friction needed (Fig. 7.23b). This happens where f/h contours converge and friction helps the flow move across f/h contours. In a flat-bottomed case, friction would be necessary all along the boundary layer in order to cross f contours(Fig. 7.23a).

The fact that the bottom pressure torque can play a more dominant role than frictional torque for the vorticity balance in the western boundary current questions the physical relevance of Stommel's model.
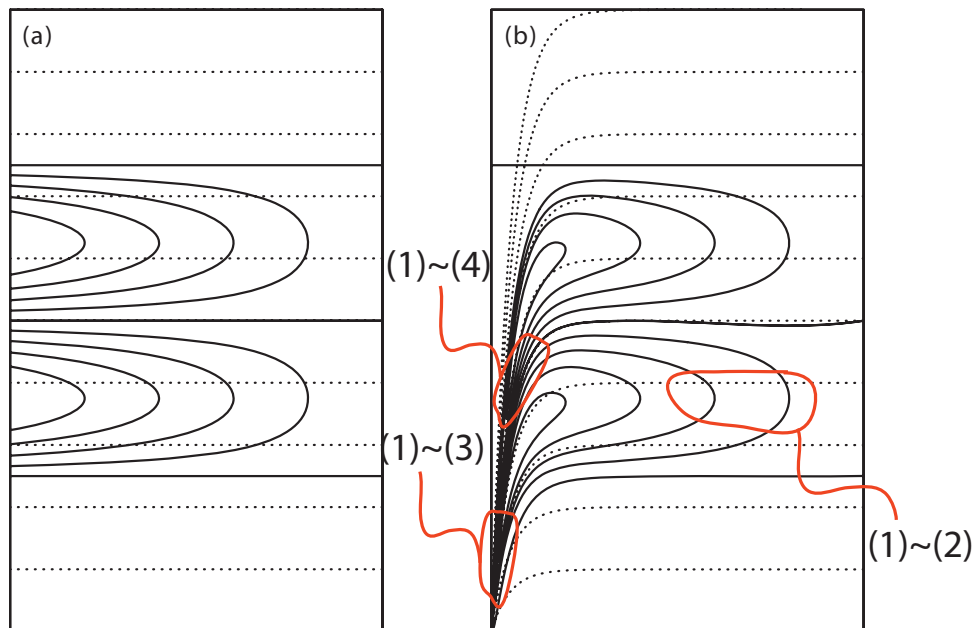
Figure 7.23: *The two-gyre Sverdrup flow for a flat-bottomed domain and a domain with sloping sidewalls. f/h contours are dotted. [adapted from Vallis (2006)].*
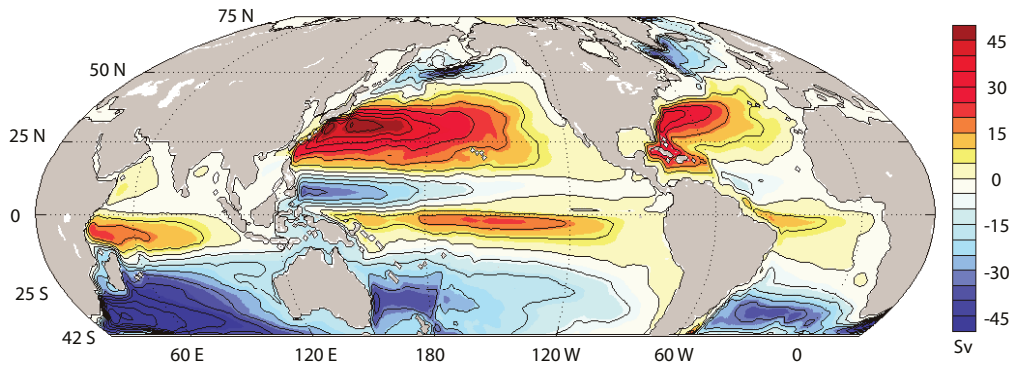
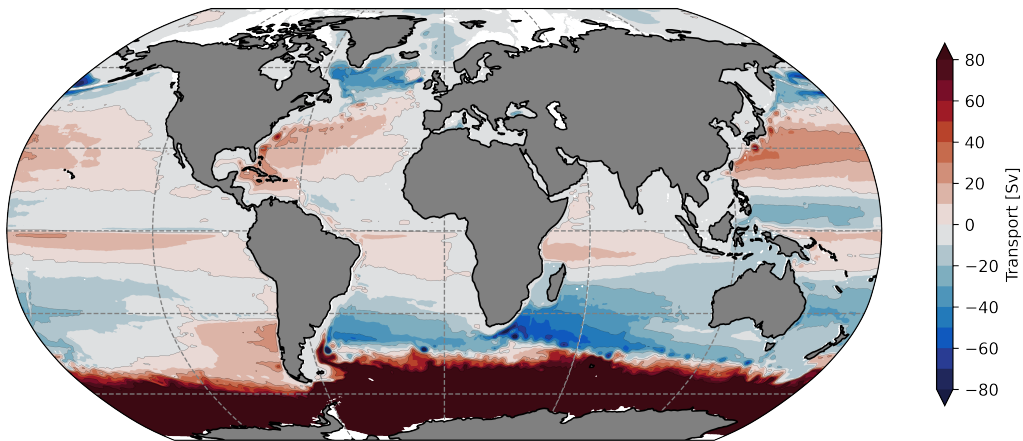Figure 7.24: *A realistic barotropic streamfunction. [adapted from Vallis (2006)].*

Figure 7.25: *The quasi-barotropic streamfunction from MOM at 0.25 degree resolution (time-mean for the period 2013-2017).*

Exercices

1. Compute the Sverdrup circulation in a rectangular ocean ($0 < x < L_x, 0 < y < L_y$) forced by a zonal wind stress

$$\tau_0^x(y) = -\tau_0 \cos\frac{\pi y}{L_y}, \quad \tau_0^y = 0.$$

Take $\tau_0 > 0$ and a constant β. Show that the Sverdrup transport velocities and the streamfunction are

$$U = -(L_x - x)\frac{\tau_0 \pi^2}{\beta L_y^2}\cos\frac{\pi y}{L_y},$$

$$V = -\frac{\tau_0 \pi}{\beta L_y}\sin\frac{\pi y}{L},$$

$$\psi(x, y) = (L_x - x)\frac{\tau_0 \pi}{\beta L_y}\sin\frac{\pi y}{L_y}.$$

Take the following parameters: L_x=5000 km, L_y=4000 km, τ_0=10^{-4}m^2 s^{-2} (the reference density ρ_0 is absorbed into the turbulent stress vector), $f = f_0 + \beta y$, with $f_0 = 7 \times 10^{-5}$ s^{-1}, $\beta = 2 \times 10^{-11}$ m^{-1}s^{-1}.

Show that the maximum transport across the basin width is $(\pi B/L)\tau_0/\beta$ and amounts to $\sim$20 Sv.
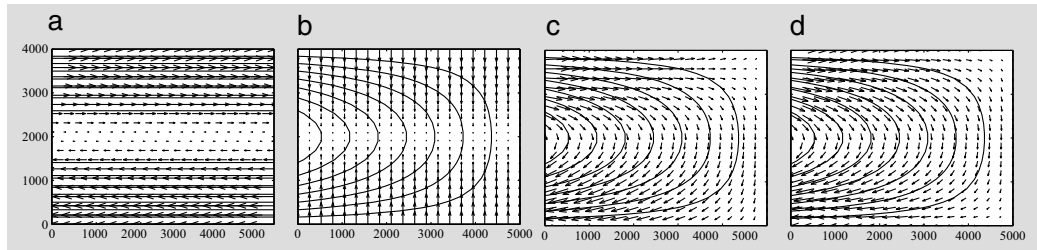
Figure 7.26: *(a) Wind stress pattern. (b) The transports due to the Ekman layer. (c) The geostrophic part with $U_g = U - U_E$, $V_g = V - V_E$ (note that $U_E = 0$). (d) The Sverdrup transport. The Sverdrup transport streamfunction ψ is shown in all plots.*

2. What happens, and why, to the transport at $\text{curl}_z\tau = 0$?

3. Compute the Ekman, geostrophic and Sverdrup transports for the following parameters. What is the total flux through the basin?

- $\theta = 35°\text{N}$
- $\tau^x = 10^{-1} \ Nm^{-2}$
- $\tau^y = 0$
- L_y =1000 km; L_x=5000 km
- f=$10^{-4} \ s^{-1}$
- $\beta = 2 \times 10^{-11} \ m^{-1}s^{-1}$

4. Compute the Sverdrup subtropical meridional transport in the North Atlantic for the given parameters. What is the typical size of the interior velocity (cm s^{-1}) if the transport is carried over the upper 1 km of the ocean and the basin is 3000 km wide?

- $\theta = 35°\text{N}$
- $\tau^x = 0.1 \ Nm^{-2}$
- $\tau^y = -0.1 \ Nm^{-2}$
- $curl_z\tau = -0.1 \times 10^{-6} \ N \ m^{-3}$
- $\rho_0 = 10^3 \ kgm^{-3}$
- $\beta = 2 \times 10^{-11} \ m^{-1}s^{-1}$

Chapter 8

Overturning Circulations

The Meridional Overturning Circulation, or MOC, of the ocean is the circulation associated with sinking mostly at high latitudes and upwelling elsewhere, with the *meridional transport mostly taking place below the main thermocline*. The theory explaining the MOC is not nearly as settled as that of the quasi-horizontal wind-driven circulation, but considerable progress has been made, in particular with a significant re-thinking of the fundamentals, especially concerning the role of the wind in maintaining a deep MOC.

That there is a deep circulation has been known for a long time, largely from observations of tracers such as temperature, salinity, and constituents such as dissolved oxygen and silica. We can also take advantage of numerical models that are able to assimilate observations (mainly from hydrographic measurements, floats and satellites) and produce a state estimate of the overturning circulation that is consistent with both the observations and the equations of motion (see Fig.8.1). We see that the water does not all upwell in the subtropics as we assumed so far in the simple thermocline scalings.

In fact, much of the mid-depth circulation more-or-less follows the isopycnals that span the two hemispheres, sinking in the North Atlantic and upwelling in the Southern Ocean, with the transport in between being, at least in part, adiabatic (see Fig.8.1).

The MOC used to be known as the 'thermohaline' circulation, reflecting the belief that it was primarily driven by buoyancy forcing arising from gradients in temperature and salinity. Such a circulation requires that the diapycnal mixing must be sufficiently large, but many measurements have suggested this is not the case and that has led to a more recent view that the MOC is at least partially, and perhaps primarily, mechan-
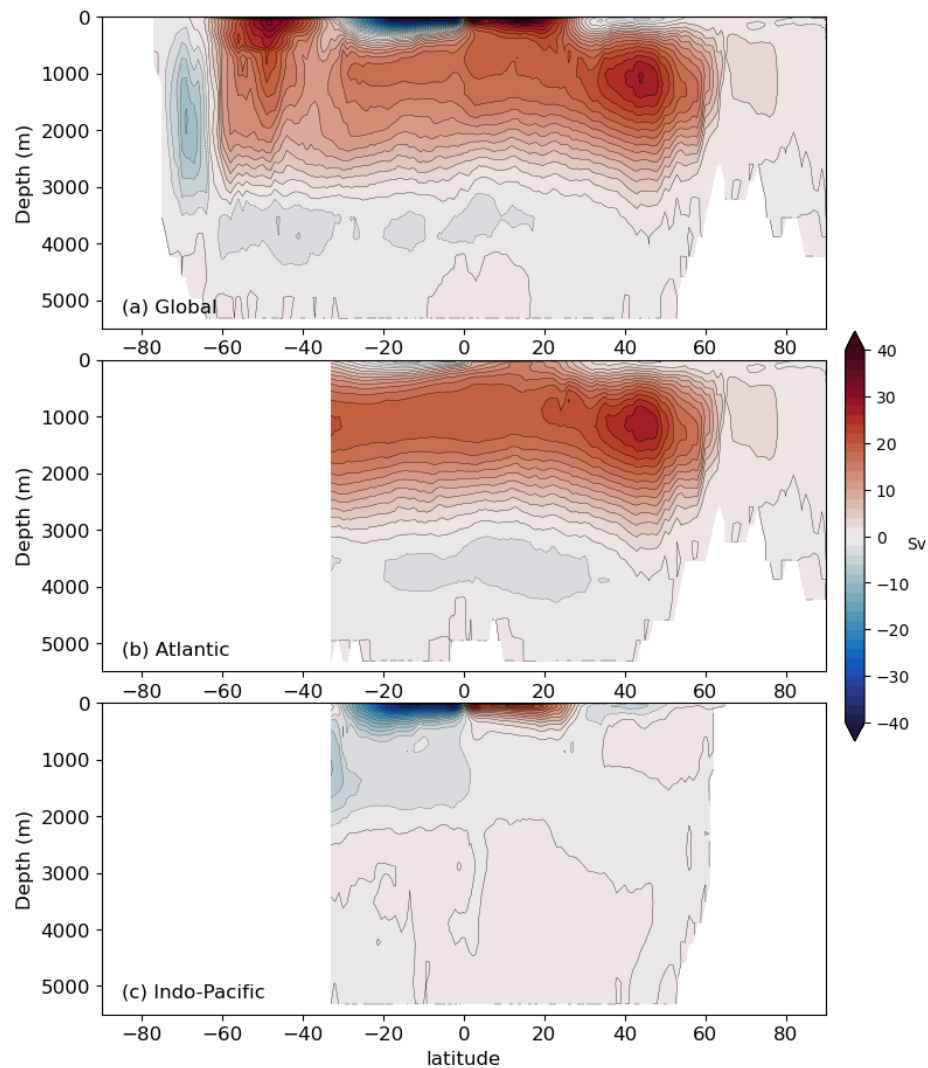
51

Figure 8.1: *The global MOC as computed from a Coupled General Circulation Model (CGCM). We clearly see the presence of the North Atlantic Deep Water cell, the interhemispheric meridional circulation, a locally-circulating deacon Cell, and two SubTropical Cells. Each meridional cell is driven by different dynamics and all together set up the global ocean circulation.*

ically driven, mostly by winds, and so *along* isopycnals instead of *across* them. However, the situation is not wholly settled, and it is almost certain that both buoyancy and wind forcing, as well as diapycnal diffusion, play a role.
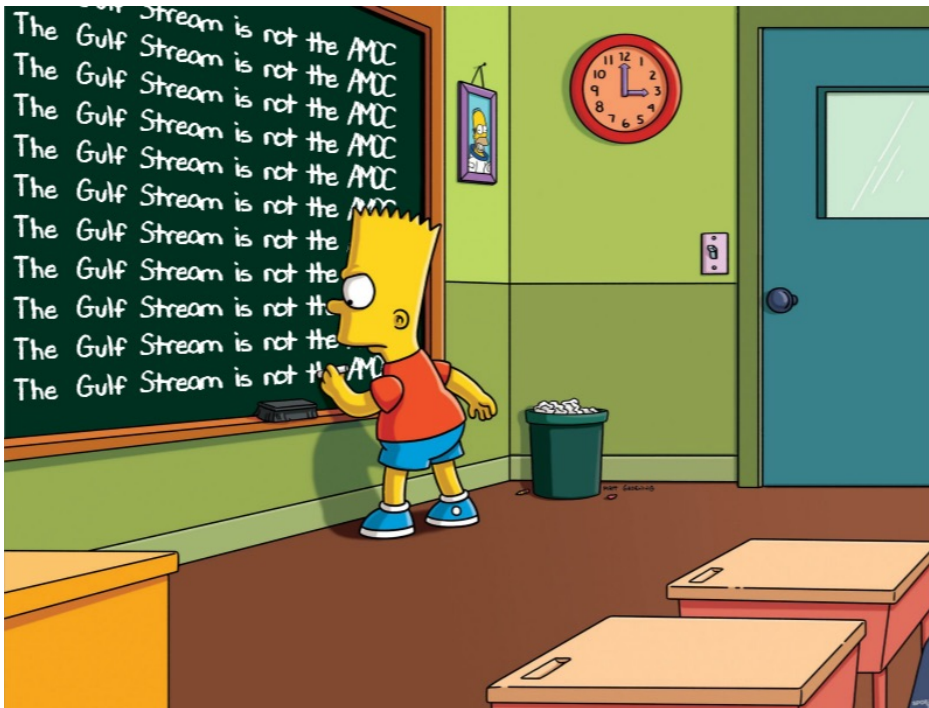
Figure 8.2: *The Gulf Stream is the western boundary current of the subtropical wind-driven gyre whereas the AMOC is part of a global meridional overturning circulation. The surface branch of the AMOC is located in the vicinity of the Gulf Stream but the two are governed by different dynamics. A possible weakening of the AMOC would not affect the Gulf Stream, which is controlled by the wind stress curl in the North Atlantic interior.*

8.1 Depth of the wind's influence and the main thermocline

We now make a first step towards understanding what sets the depth at which reaches the influence of the wind-driven circulation. How deep is the wind's influence?

8.1.1 Munk's hypotesis

What is actually giving rise to the observed density structure of the upper ocean? in particular to the main thermocline (yes, there are more thermocline regimes ... but we will leave those for another day ...).

Supposing there is net surface warming at low latitudes and net cooling at high latitudes, this will maintain a meridional temperature gradient at the surface. We can thus presume that there will be water rising at the surface at low latitudes and then returning to polar regions where they sink. The dynamics of this meridional overturning circulation (MOC) will set a balance between upward motion and downward diffusion, responsible for the depth at which density (or in this case temperature) will change very rapidly in the vertical.

After cold water has sinked at high latitudes, this will create, through hydrostasy, a higher pressure in the deep ocean at high latitudes than at low latitudes, where the water is much warmer. *For this reason the bottom water will move equatorward and fill the abyss.* As this water moves it is warmed by heat diffusion from above (diffusion is directed downwards), keeping the circulation going. There is thus a vertical density(temperature) gradient throughout the basin but in the polar regions where cold water sinks.

Given the simple cartoon depicting the ocean, with polar waters upwelling into a region of warmer water, we can consider a simple advective-diffusive balance. Munk (1966) hypothesized that the below 1000 m the flow obeys the vertical advection-diffusion equation, i.e. we can neglect horizontal transports of temperature and salinity.

$$w\frac{\partial T}{\partial z} = K_v \frac{\partial^2 T}{\partial z^2} \tag{8.1}$$

where w is the vertical velocity, K_v an eddy vertical diffusivity and T the temperature. w is positive, towards the surface, and diffusion is directed downwards, producing a balance between the two circulations.

If w and K_v are constants, $T = T_T$ at $z = 0$ and $T = T_B$ at $z = -\infty$, we get

$$T = (T_T - T_B)\, e^{zw/K_v} + T_B. \tag{8.2}$$

The temperature falls exponentially away from the surface. The scale of the exponential decay is

$$\boxed{\delta = \frac{K_v}{w}}. \tag{8.3}$$

This is an estimate of the thickness of the thermocline. Munk fitted temperature and salinity data from the central Pacific with these functions to estimate Kv. The central Pacific is a good place because it has low horizontal velocities in the deep ocean. Munk obtained values of $K_v \sim 1.3 \times 10^{-4}$ m^2 s^{-1}.

If we use $w = 10^{-7}$ m s^{-1} and a range of diffusivity K_v between 10^{-4} and 10^{-5} m^2 s^{-1}, we get an e-folding vertical scale between δ=100 m and 1000 m. The first case is too shallow, but the second is closer to observations. According to Munk's recipe, the upwelling of deep waters is driven by downward diffusion of heat from the surface and the simple model predicts that the temperature gradient is concentrated in the upper ocean.

Cold water is upwelling and only needs to warm up as it approaches the warm upper surface. If K_v were very very small there would just be a
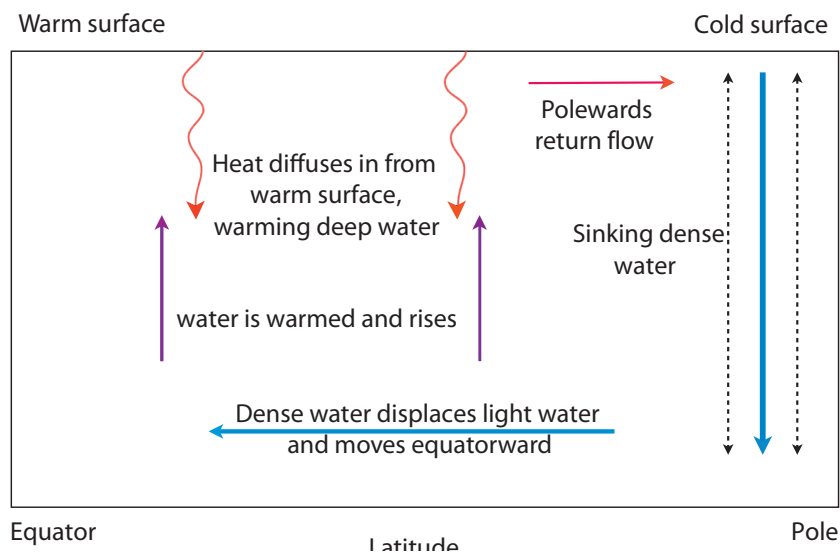

Figure 8.3: *Schematic of a single-celled meridional overturning circulation. Sinking is concentrated at high latittude and upwelling spread out over lower latitudes. [from Vallis (2006)]*

thin boundary layer at the top of the ocean, and the overturning circulation would be very weak because almost the entire ocean would be as dense as the cold polar surface waters.

8.1.2 Scaling and dynamics of the main thermocline

The flow, which has a small Rossby number and very large scale of motion, obeys the planetary-geostrophic equations

$$f \times u = -\nabla \phi, \tag{8.4}$$

$$\frac{\partial \phi}{\partial z} = b, \tag{8.5}$$

$$\nabla \cdot v = 0, \tag{8.6}$$

$$\frac{\mathrm{D} b}{\mathrm{D} t} = \kappa \frac{\partial^2 b}{\partial z^2}. \tag{8.7}$$

Which are the momentum equations, hydrostasy, continuity and the thermodynamics equations respectively. These equations hold for the interior
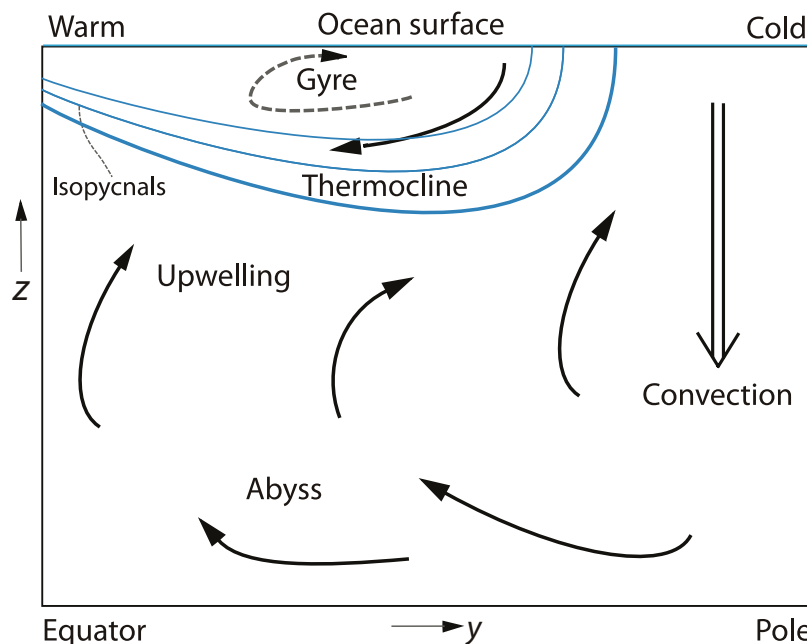
Figure 8.4: *Wind forcing in the subtropics pushes the warm surface water into the fluid interior, deepening the thermocline as well as circulating as a gyre. [from Vallis (2006)]*

flow, below the Ekman layer, and we insert the effects of the wind stress by specifying a vertical velocity W_E.

A diffusive scale

Suppose there is no wind forcing, and the only possible driver of the circulation is diffusivity: what would be the depth of the *diffusive thermocline* in the subtropical gyre?

We again use the approximation of an advective-diffusive balance. We take the curl of the momentum equations and use mass continuity to obtain the linear vorticity equation. We take the vertical derivative of the momentum equation and use hydrostasy to obtain the thermal wind:

$$w\frac{\partial b}{\partial z} = \kappa\frac{\partial^2 b}{\partial z^2}, \quad \beta v = f\frac{\partial w}{\partial z}, \quad f\frac{\partial \boldsymbol{u}}{\partial z} = \boldsymbol{k} \times \nabla b \tag{8.8}$$

and their scales are

$$\frac{W}{\delta} = \frac{\kappa}{\delta^2}, \quad \beta U = f\frac{W}{\delta}, \quad f\frac{U}{\delta} = \frac{\Delta b}{L} \tag{8.9}$$

The first scaling is the same as the first diffusive scaling (Munk's abyssal recipes) we have previously obtained ($\delta = \kappa/w$). But the previous scale did not have any information on the vertical velocity, which can now be obtained from the second and third scaling:

$$W = \frac{\beta U \delta}{f} \quad \text{and} \quad U = \frac{\Delta b \delta}{fL} \quad \text{gives} \quad W = \frac{\beta \delta^2 \Delta b}{f^2 L}. \tag{8.10}$$

This inserted into the scale for δ leads to a scale for the thickness

$$\delta = \left(\frac{\kappa f^2 L}{\beta \Delta b}\right)^{1/3} \tag{8.11}$$

and using the above to find a scale for W leads to

$$\boxed{W = \left(\frac{\kappa^2 \beta \Delta b}{f^2 L}\right)^{1/3}} \tag{8.12}$$

Some typical values for a subtropical gyre are

$$\Delta b = 10^{-2} m\,s^{-2}$$
$$L = 5000\,km$$
$$f = 10^{-4} s^{-1}$$
$$\kappa = 10^{-5} m^2\,s^{-2}$$

and these values give us:

$$\delta = \left(\frac{10^{-5} \times 10^{-8} \times 5 \times 10^6}{10^{-11} 10^{-2}} \right)^{1/3} \approx 150 \, m \qquad (8.13)$$

$$W = \left(\frac{10^{-10} \times 10^{-11} \times 10^{-2}}{10^{-8} \times 5 \times 10^6} \right)^{1/3} \approx 10^{-7} \, m\,s^{-1} \qquad (8.14)$$

This vertical velocity is too small. The observed values of Ekman pumping velocities are on the order of 10^{-6}–10^{-5} m s^{-1}. Using $\kappa = 10^{-5} m^2 s^{-2}$, which is too large!, would result in $\delta \approx 700 \, m$ and $W \approx 4.6 \times 10^{-7} \, m\,s^{-1}$.

The diffusive scaling is not sufficient and we will now build an adiabatic scaling estimate for the depth of the wind's influence.

An advective scale

Since the diffusive scaling is providing a vertical velocity much smaller than the Ekman pumping velocity at the top of the ocean, we conclude that we can ignore the diffusive term and the thermodynamic term completely, and construct an adiabatic scaling estimate for the depth of the wind's influence. Also, in subtropical gyres the Ekman pumping is downward, and the diffusive velocity is upward. This implies that at some level, D, we expect the vertical velocity to be zero.

The equation of motion are just thermal wind balance and linear geostrophic vorticity equation:

$$\beta v = f \frac{\partial w}{\partial z}, \quad f \frac{\partial \boldsymbol{u}}{\partial z} = \boldsymbol{k} \times \nabla b \qquad (8.15)$$

and their scales are

$$\beta U = f \frac{W}{D}, \quad \frac{U}{D} = \frac{\Delta b}{fL}. \qquad (8.16)$$

We take the vertical velocity to be that due to Ekman pumping, W_E The depth scale of motion is thus

$$\boxed{D = \left(\frac{W_E f^2 L}{\beta \Delta b} \right)^{1/2}.} \qquad (8.17)$$

If we relate U and W_E using mass conservation ($U/L = W_E/D$), instead of the Sverdrup balance, then

$$D = \left(\frac{W_E f L^2}{\Delta b} \right)^{1/2}.$$ (8.18)

The above estimate predicts a depth of the wind-influenced region (1) increasing with the magnitude of the wind stress (since $W_E \propto curl_z \tau$) and (2) decreasing with the meridional temperature gradient. The second dependency arises because a larger temperature gradient increases the thermal wind shear. Given that the horizontal transport (UD) is fixed by mass conservation, the only way that these two can remain consistent is for the vertical scale to decrease.

Taking $W_E = 10^{-6}$ m s^{-1} or $W_E = 10^{-5}$ m s^{-1}, what would be the depth of the wind-influenced region D? You will see that in both cases the estimate suggests that the wind-driven circulation is an upper ocean phenomenon ($\sim$500 m).

- The wind-influenced scaling D is the depth to which the directly wind-driven circulation can be expected to penetrate.

- Over the depth D we expect to see wind-driven gyres

- Below D lies the abyssal circulation, which is not wind-driven in the same way (but somehow it is ...)

- The thickness δ is the diffusive transition region between two different water masses: a warm subtropical water within the wind-driven layer and a cold dense water upwelling from the abyss.

- D is the depth of the thermocline. δ is the thickness of the thermocline (Fig. 8.5).
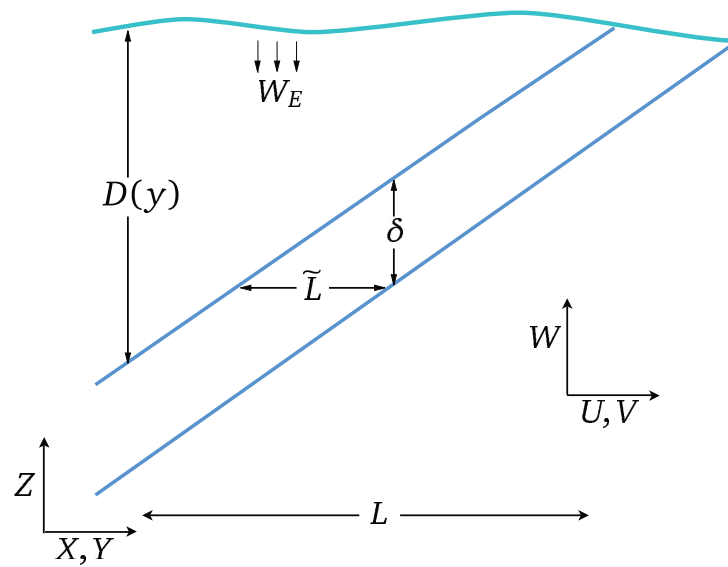
Figure 8.5: *Scaling of the thermocline. The diagonal lines mark the diffusive thermocline of thickness δ and depth D(y). [from Vallis (2006)]*

8.2 A model for the oceanic abyssal flow: The Stommel-Arons model

In Munk's hypothesis, waters that fill the deep ocean can only return to the sea surface as a result of diapycnal eddy diffusion of buoyancy (heat and freshwater) downward from the sea surface. Munk's (1966) diapycnal eddy diffusivity estimate of $\kappa_v = 1 \times 10^{-4}\,\mathrm{m^2\,s^{-1}}$ was based on the idea of isolated sources of deep water and widespread diffusive upwelling of this deep water back to the surface. From all of the terms in the temperature and salt equations, Munk assumed that most of the ocean is dominated by the balance between vertical advection (upwards) and vertical diffusion (downwards; as in the diffusive thermocline):

$$w\frac{\partial T}{\partial z} = \kappa_v \frac{\partial^2 T}{\partial z^2}. \tag{8.19}$$

Munk obtained his diffusivity estimate of $10^{-4}\,\mathrm{m^2\,s^{-1}}$ from an average temperature profile and an estimate of about 1 cm/day for the upwelling velocity w, which can be based on deep-water formation rates and an assumption of upwelling over the whole ocean. But, the observed diapycnal eddy diffusivity in the open ocean away from boundaries is an order of magnitude smaller than Munk's estimate!. This means that there must be much larger diffusivity in some regions of the ocean – now thought to be at the boundaries, at large seamount and island chains, and possibly the equator. And, this also means that mechanical forcing must play a fundamental role in bringing large fraction of the water back to the surface.
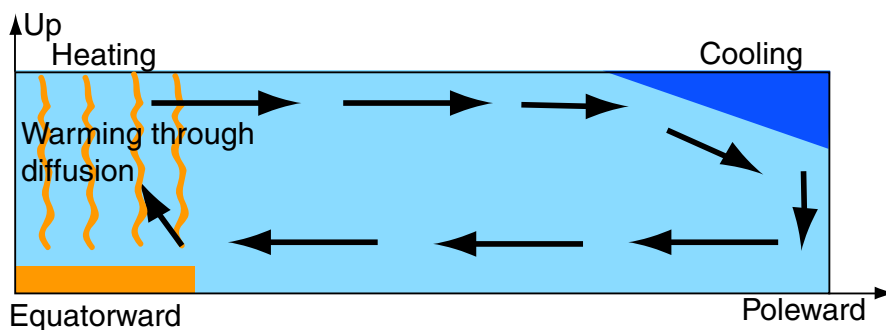

Figure 8.6: *The role of vertical (diapycnal) diffusion in the MOC, replacing a deep tropical warm source with diapycnal diffusion that reaches below the effect of high latitude cooling. [from Talley et al. (2011)]*

We will model the deep ocean as a single layer of homogeneous fluid in which there is a localized injection of mass at high latitudes (S_o), representing convection. Mass is extracted from this layer by upwelling into the warmer waters above it, keeping the average thickness of the abyssal layer constant. We assume that this upwelling is nearly uniform, that the ocean is flat-bottomed, and that a passive western boundary current may be invoked to satisfy mass conservation, and which does not a affect the interior flow.

The planetary geostrophic momentum equations and mass continuity are

$$f \times u = -\nabla_z \phi \quad \nabla_z \cdot u = 0. \tag{8.20}$$

Eliminating the pressure terms yields the vorticity balance

$$\beta v = f \frac{\partial w}{\partial z}. \tag{8.21}$$

The vertical velocity is positive and uniform at the top and zero at the bottom of the lower layer:

$$\beta v = f \frac{w_0}{H} \tag{8.22}$$

where w_0 is the uniform upwelling velocity and H is the layer thickness. The last equations tells us that, since by assumption $w_0 > 0$ (stretching of water columns), $v > 0$ and the flow is polewards everywhere and vanishing at the equator. The model is similar to the wind-driven circulation, but
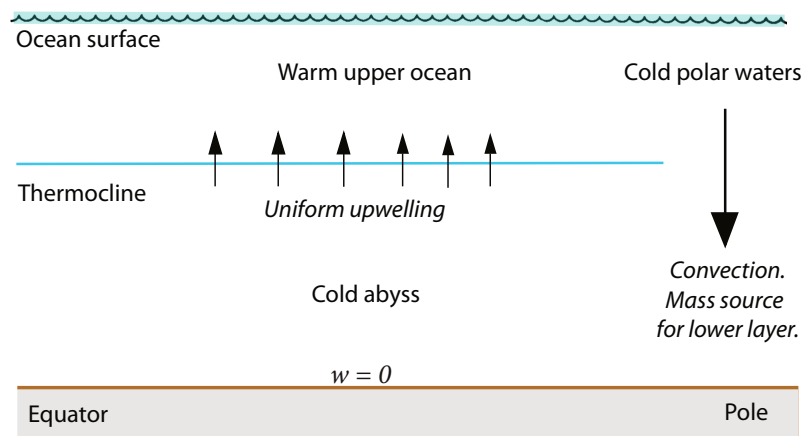

Figure 8.7: *Stommel-Arons ocean model of the abyssal circulation. Convection at high latitudes provides a localized mass-source to the lower layer, and upwelling through the thermocline provides a more uniform mass sink. [from Vallis (2006)]*

in the wind-driven case w_0 is the Ekman pumping. Here, it is the imposed uniform upwelling.

By geostrophic balance we have that

$$v = \frac{1}{f}\frac{\partial \phi}{\partial x} \tag{8.23}$$

so that the pressure is given by

$$\phi = -\int_{x}^{x_e} \left(\frac{f^2 w_0}{\beta H}\right) dx' = -\frac{f^2}{\beta H} w_0 (x_e - x) \tag{8.24}$$

assuming the boundary condition that $\phi = 0$ at $x = x_e$.

Using again geostrophic balance for the zonal velocity

$$u = -\frac{1}{f}\frac{\partial \phi}{\partial y} = \frac{1}{f}\frac{\partial}{\partial y}\left[\frac{f^2}{\beta H} w_0 (x_e - x)\right] = \frac{2}{H} w_0 (x_E - x). \tag{8.25}$$

Remembering that $\frac{\partial f}{\partial y} = \beta$ and $\frac{\partial \beta}{\partial y} = 0$.

This result is telling us that the zonal velocity is eastward, and independent of f and latitude y.

Are we conserving mass?

$$\frac{\partial u}{\partial x} + \frac{\partial v}{\partial y} + \frac{\partial w}{\partial z} = \frac{\partial}{\partial x}\left[\frac{2}{H} w_0 (x_E - x)\right] + \frac{\partial}{\partial y}\left[\frac{f w_0}{\beta H}\right] + \frac{w_0}{H} \tag{8.26}$$

$$= -\frac{2}{H} w_0 + \frac{w_0}{H} + \frac{w_0}{H} = 0 \tag{8.27}$$

8.2.1 A sector ocean

So far we have considered the effect of a uniform upwelling velocity, inducing a poleward flow. Let's now take a few steps toward a more realistic oceanic condition in which sources and sinks exist in the abyssal layer.

In our sector ocean, or rectangle in cartesian coordinates (Fig.8.13), we have a mass source at the northern boundary, balanced by uniform upwelling. Since the interior flow will be northwards, we anticipate a southwards flowing western boundary current to balance mass. Conservation of mass in the area polewards of a latitude y demands that

$$S_0 + T_I(y) - T_W(y) - U(y) = 0, \tag{8.28}$$

where S_0 is the strength of the source, T_W the equatorwards transport within the western boundary layer, T_I the polewards transport in the interior, and U is the integrated loss due to upwelling polewards of y.

Using Sverdrup balance, $v = (f/\beta)w_0/H$, the polewards transport through the section at latitude y is

$$T_I = \int_{x_W}^{x_E} vH \, dx = \int_{x_W}^{x_E} \frac{f}{\beta} w_0 \, dx = \frac{f}{\beta} w_0 (x_E - x_W). \tag{8.29}$$

The loss through upwelling is

$$U = \int_{x_W}^{x_E} \int_y^{y_N} w_0 \, dxdy = w_0(x_E - x_W)(y_N - y). \tag{8.30}$$
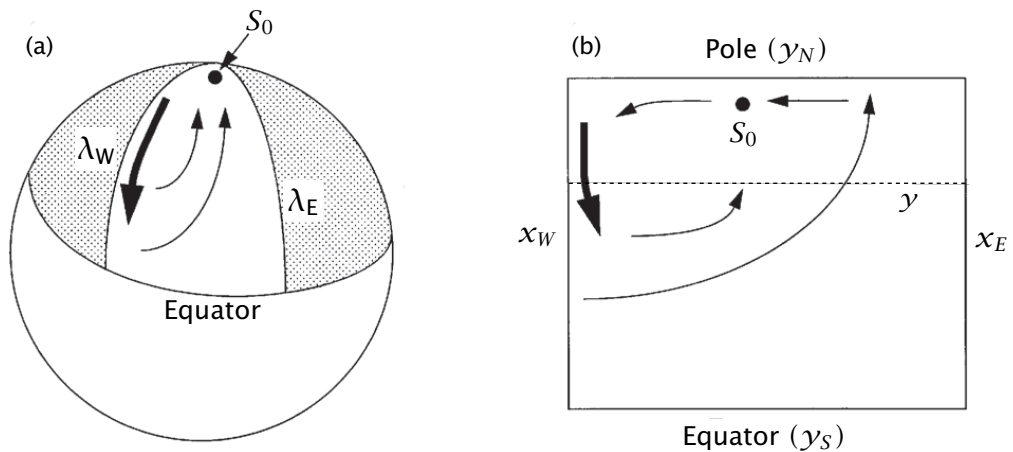

Figure 8.8: *Abyssal circulation in a spherical sector and in a corresponding Cartesian rectangle. [from Vallis (2006)]*
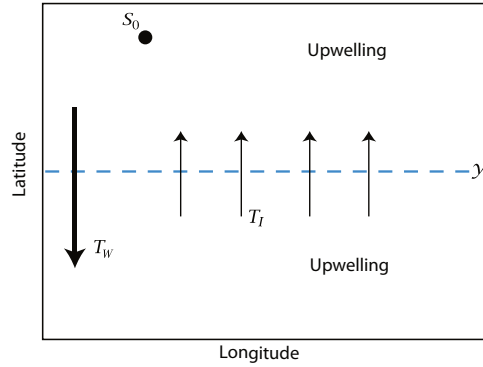
Figure 8.9: *Mass budget in an idealized abyssal ocean. Polewards of some latitude y, the mass source (S_0) plus the poleward mass flux across y (T_I) are equal to the sum of the equatorward mass flux in the western boundary current (T_W) and the integrated loss due to upwelling (U) polewards of y. [from Vallis (2006)]*

We can now estimate the strength of the western boundary current by using the two previous results:

$$T_W(y) = S_0 + T_I(y) - U(y) = S_0 + \frac{f}{\beta}w_0(x_E - x_W) - w_0(x_E - x_W)(y_N - y).$$
(8.31)

There is now a relationship we can use, ensuring mass balance over the entire basin, between sources S_0 and sinks U

$$S_0 = w_0 \Delta x \Delta y,$$
(8.32)

where $\Delta x = x_E - x_W$, and $\Delta y = y_N - y_S$.

$$T_W(y) = S_0 + \frac{f}{\beta}w_0\Delta x - w_0\Delta x(y_N - y)$$
(8.33)

$$T_W(y) = w_0\Delta x(y_N - y_S) + \frac{f}{\beta}w_0\Delta x - w_0\Delta x(y_N - y)$$
(8.34)

$$T_W(y) = w_0\Delta x\left(y - y_S + \frac{f}{\beta}\right).$$
(8.35)

Polewards of some latitude y, the mass source (S_0) plus the poleward mass flux across y (T_I) are equal to the sum of the equatorward mass flux in the western boundary current (T_W) and the integrated loss due to upwelling (U) polewards of y.

Given that y_S is our equator, we can set $y_S = 0$ and since $f = f_0 + \beta y$, we get

$$T_W(y) = w_0 \Delta x \left(2y + \frac{f_0}{\beta} \right). \tag{8.36}$$

Using mass balance $w_0 = \frac{S_0}{\Delta x y_N}$

$$T_W(y) = \frac{S_0}{y_N} \left(2y + \frac{f_0}{\beta} \right). \tag{8.37}$$

Now suppose the equatorial boundary of our domain is *at* the equator, which is what we have been thinking so far anyway, then $f_0 = 0$ and

$$\boxed{T_W(y) = 2S_0 \frac{y}{y_N}} \tag{8.38}$$

which at the northern boundary takes the form

$$T_W(y = y_N) = 2S_0. \tag{8.39}$$

> A few conclusions so far
>
> 1. At the northern boundary the equatorward transport in the western boundary current is equal to twice the strength of the source!
>
> 2. The western boundary current is equatorwards everywhere.
>
> 3. The northward mass flux at the northern boundary ($f = \beta y_N$) is equal to the strength of the source itself, given that
>
> $$T_I(y_N) = \frac{f}{\beta} w_0 \Delta x = \frac{f}{\beta} \frac{S_0}{y_N \Delta x} \Delta x = \frac{\beta y_N}{\beta} \frac{S_0}{y_N} = S_0. \tag{8.40}$$

The fact that convergence at the pole balances T_W and S_0 does not of course depend on the particular choice we made for f and y_S. The flow pattern evidently has the property of recirculation (see Fig.8.10 and Fig.8.11): this is one of the most important properties of the solution, and one that is likely to transcend all the limitations inherent in the model. This single-hemisphere model may be thought of as a crude model for aspects of the abyssal circulation in the North Atlantic, in which convection
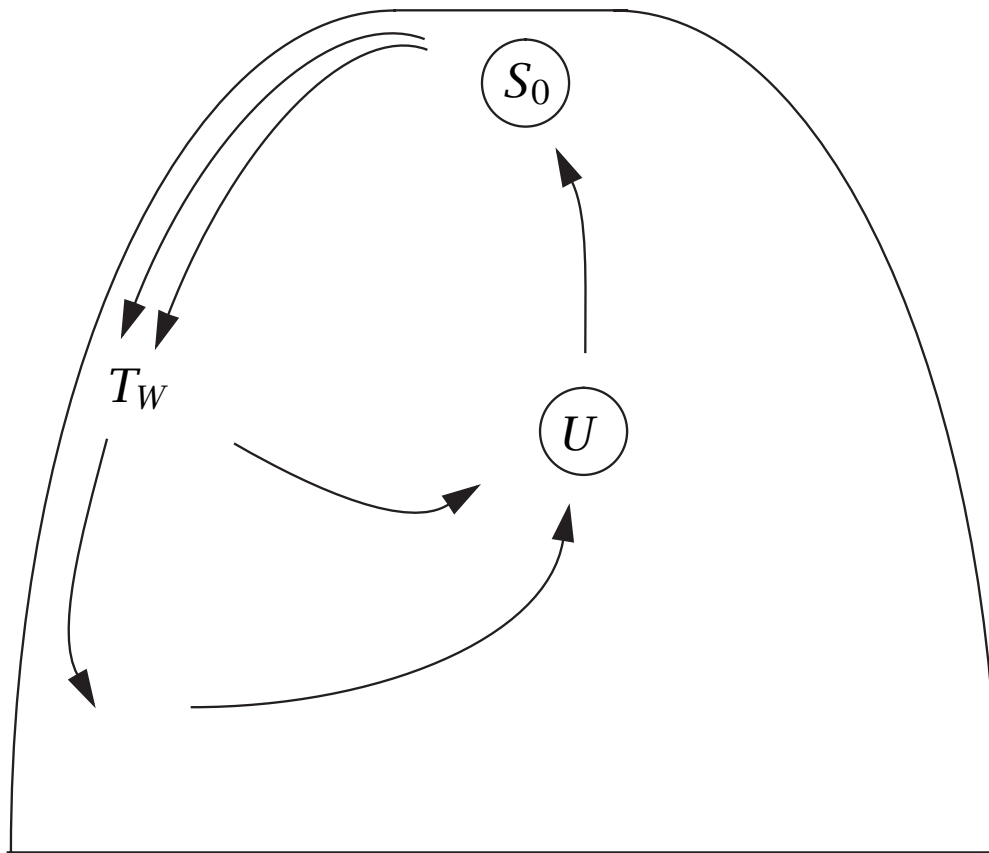
Figure 8.10: *Schematic of a Stommel–Arons circulation in a single sector. The transport of the western boundary current is greater than that provided by the source at the apex, illustrating the property of recirculation. The transport in the western boundary current T_W decreases in intensity equatorwards, as it loses mass to the polewards interior flow, and thence to upwelling. The integrated sink, due to upwelling, U, exactly matches the strength of the source, S_0. [from Vallis (2006)]*

at high latitudes near Greenland is at least partially associated with the abyssal circulation.

The model can be expanded to a two-hemisphere basin, showing that a mass source in the Southern Hemisphere can drive deep recirculation in the opposite hemisphere. Later, a global map can be constructed with this simple model, qualitatively explaining deep circulation in the world oceans (Fig.8.12).

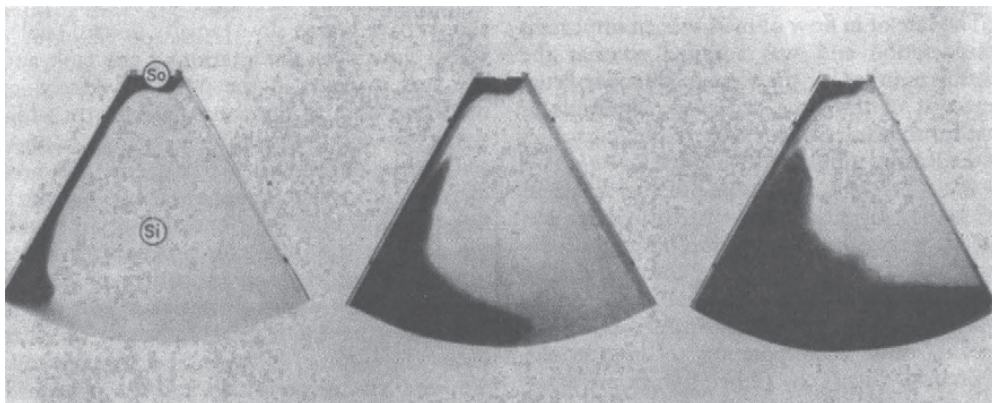Perhaps the greatest success of the model is that it introduces the no-
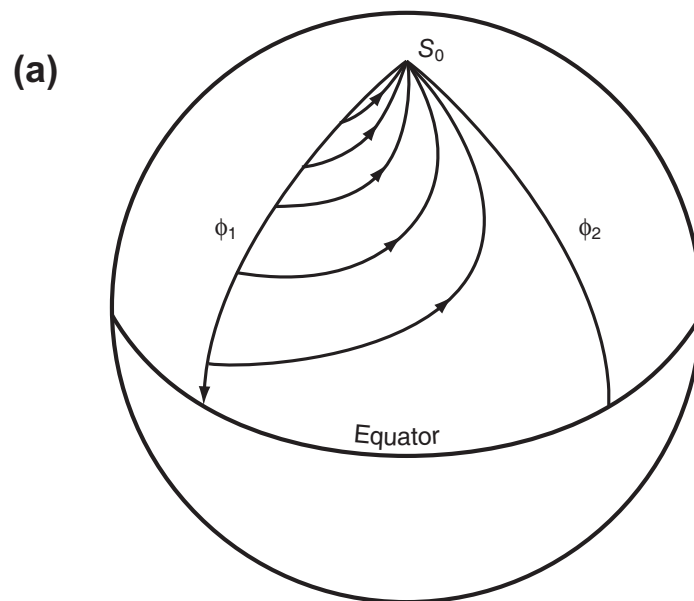
Figure 8.11: *(a) Abyssal circulation model. After Stommel and Arons (1960a). (b) Laboratory experiment results looking down from the top on a tank rotating counterclockwise around the apex (S_0) with a bottom that slopes towards the apex. There is a point source of water at S_0. The dye release in subsequent photos shows the Deep Western Boundary Current, and flow in the interior S_I beginning to fill in and move towards S_0. [from Talley et al. (2011)]*

tions of deep western boundary currents and recirculation – enduring concepts of the deep circulation that remain with us today. **This is a singular case in which a theoretical study predicted a major ocean current before it was actually observed!**. For example, the North Atlantic ocean does
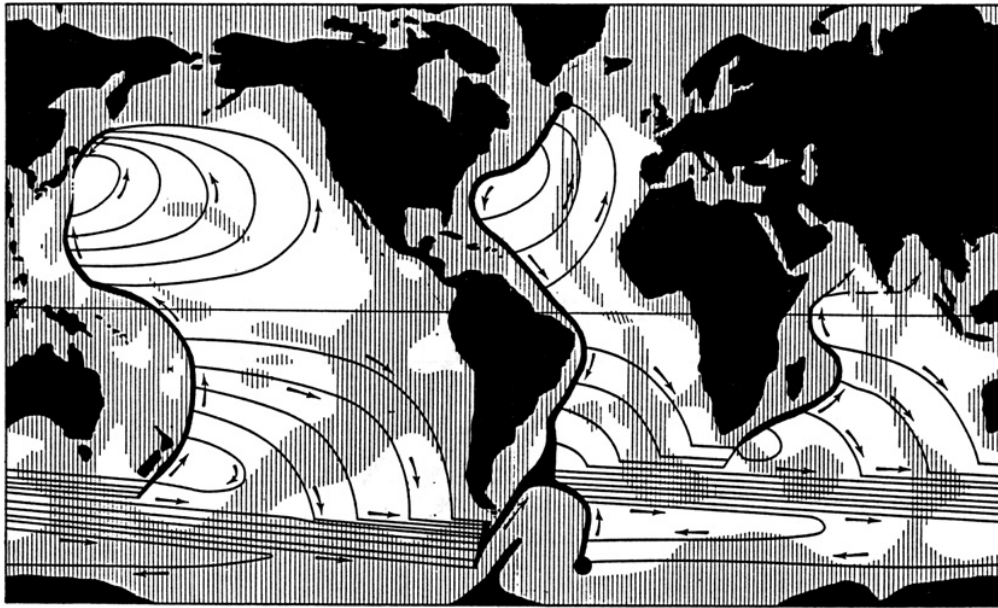
Figure 8.12: *Global abyssal circulation model, assuming two deep water sources (filled circles near Greenland and Antarctica). [from Talley et al. (2011)]*

have a well-defined deep western boundary current running south along the eastern seaboard of Canada and the United States. However, in other important aspects the model is found to be in error, in particular it is found that there is little upwelling through the main thermocline – much of the water formed by deep convection in the North Atlantic in fact upwells in the Southern Hemisphere.

An important assumption is that of uniform upwelling, across isopycnals, into the upper ocean, and that $w = 0$ at the ocean (flat) bottom. When combined with the linear geostrophic vorticity balance in the ocean abyss $\beta v = f \frac{\partial w}{\partial z}$, this gives rise to a poleward interior flow, and by mass conservation a deep western boundary current. The upwelling is a consequence of a finite diffusion, which in turn leads to deep convection as in the model of sideways convection. In reality, the deep water might not upwell across isopycnals at all, but might move along isopycnals that intersect the surface (or are connected to the surface by convection). If so, then in the presence of mechanical forcing a deep circulation could be maintained even in the absence of a diapycnal diffusivity. The circulation might then be qualitatively different from the Stommel–Arons model, although a linear vorticity balance might still hold, with deep western boundary currents.

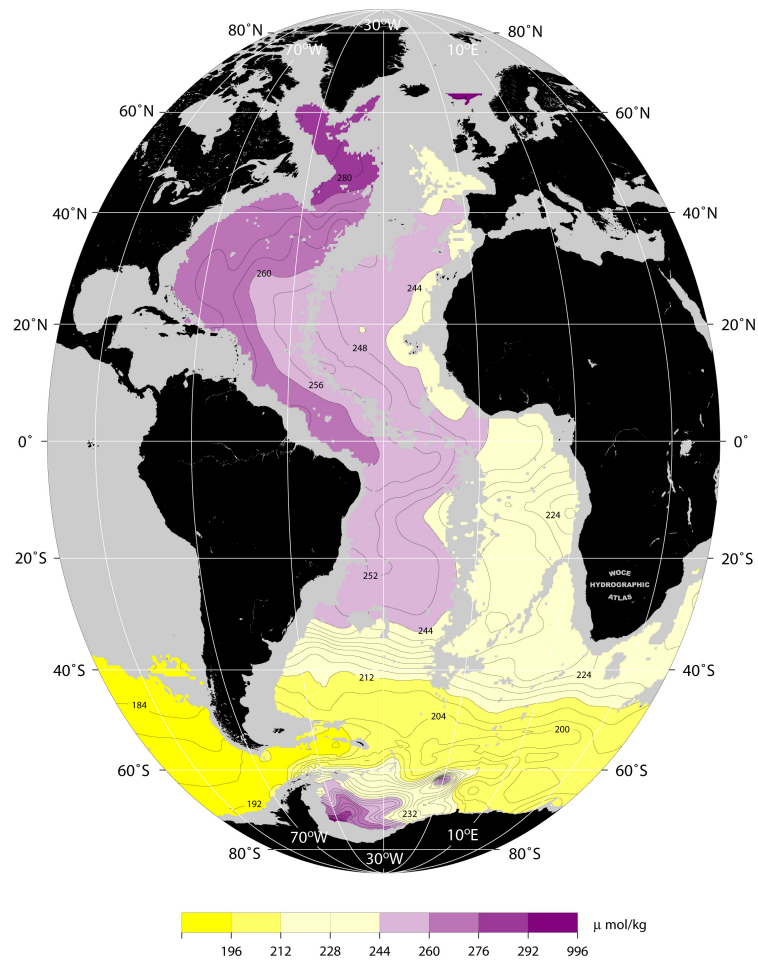**Oxygen on the Neutral Surface γ^n=28.10**

Figure 8.13: *One feature of the solution is a deep western boundary current that flows southward in the Atlantic Ocean. This is consistent with observations. For example, high oxygen water is formed in the North Atlantic and flows southward in the deep western boundary current. [from the WOCE Atlas]*

8.3 Wind-driven Overturning

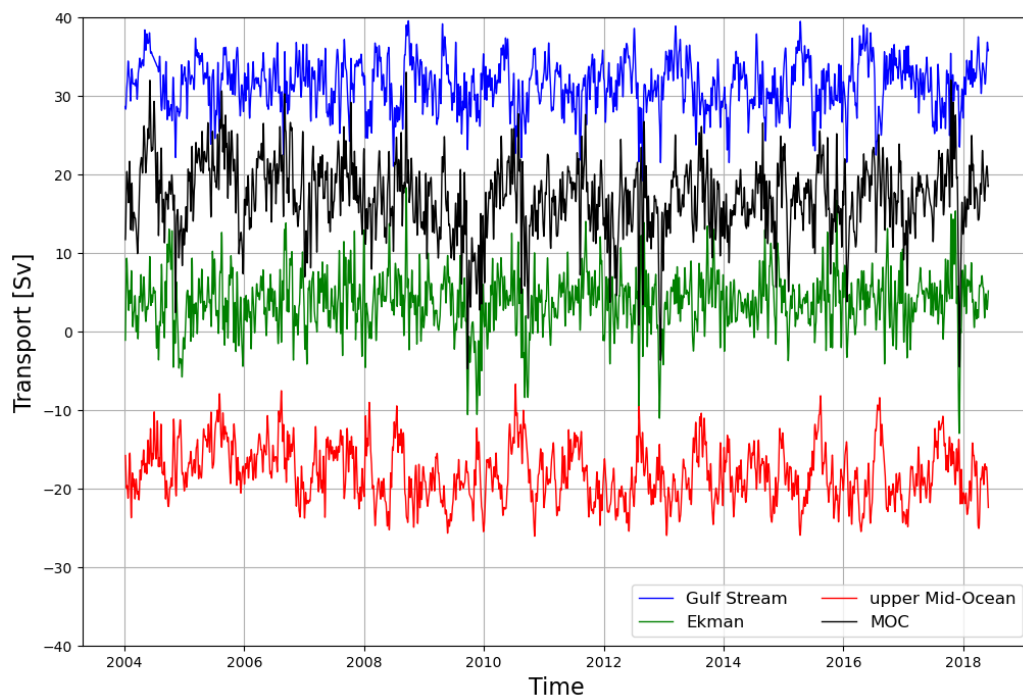Notes will be written soon. For now, please look at the slides shown in class.

Figure 8.14: *Time series of different components of volume transports from the RAPID Array (2004-2019).*
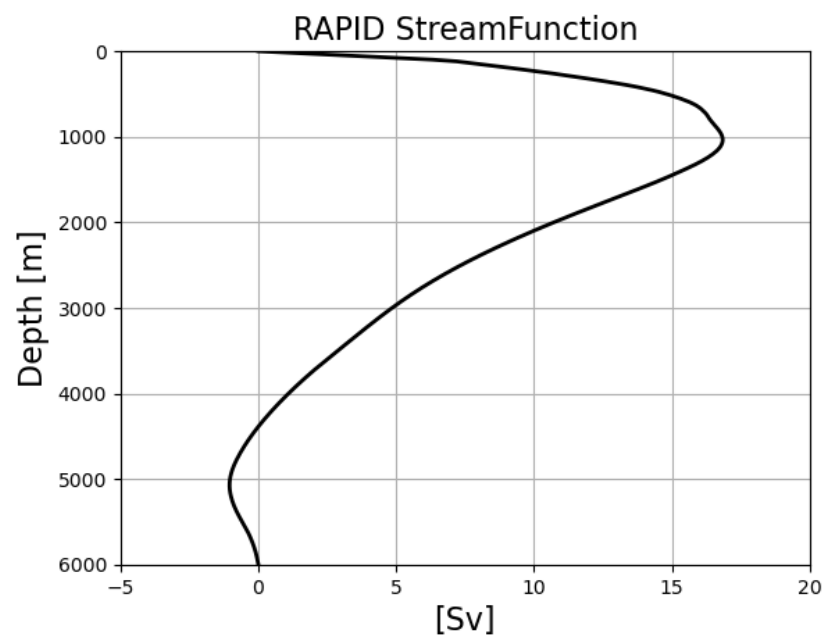
Figure 8.15: *Time mean (2004-2019) of the overturning stream function at 26.5N from RAPID.*

Bibliography

Olbers, D., J. Willebrand, and C. Eden, *Ocean Dynamics*, Springer-Verlag, 704 pp, 2012.

Talley, L., G. L. Pickard, W. J. Emery, and J. H. Swift, *Descriptive Physical Oceanography*, Academic Press, 560 pp, 2011.

Vallis, G. K., *Atmospheric and Oceanic Fluid Dynamics*, Cambridge Univ. Press, 745 pp, 2006.